CHALMERS
UNIVERSITY OF TECHNOLOGY

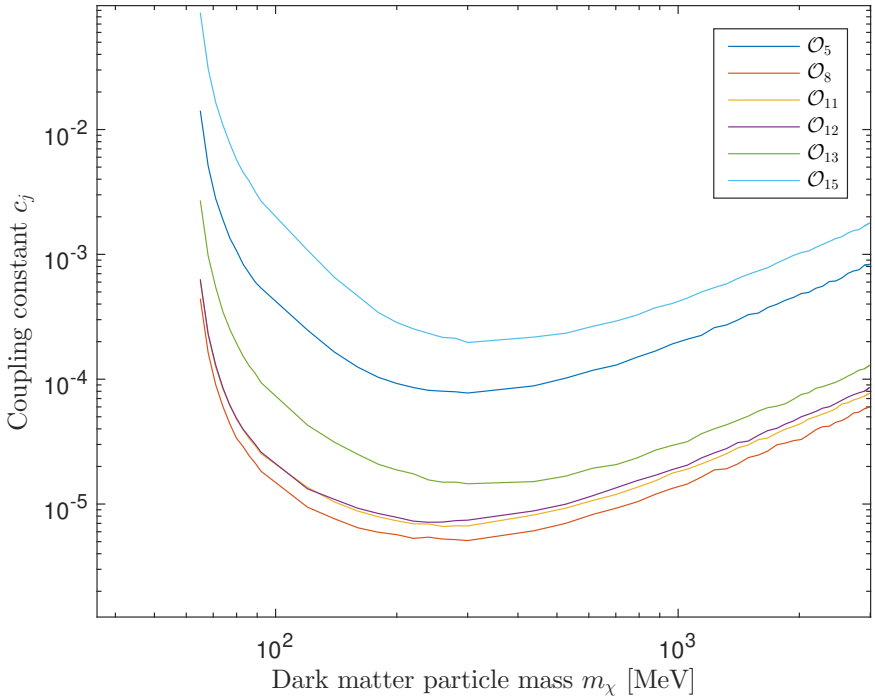

Prospects for the Discovery of General Dark Matter-Induced Atomic Responses

Finding the Statistical Significance for Signal Discovery of Future Experiments

Master's thesis in Physics and Astronomy

OSKAR LINDROOS

Department of Physics
CHALMERS UNIVERSITY OF TECHNOLOGY
Gothenburg, Sweden 2020

Master's thesis 2020:TIFX05

Prospects for the Discovery of General Dark Matter-Induced Atomic Responses

Finding the Statistical Significance for Signal Discovery of Future Experiments

OSKAR LINDROOS

CHALMERS
UNIVERSITY OF TECHNOLOGY

Department of Physics
Division of Subatomic, High Energy and Plasma Physics
Dark Matter Research Group
Chalmers University of Technology
Gothenburg, Sweden 2020

Prospects for the Discovery of General Dark Matter-Induced Atomic Responses
Finding the Statistical Significance for Signal Discovery of Future Experiments
OSKAR LINDROOS

Supervisor: Riccardo Catena, Department of Physics
Examiner: Christian Forssén, Department of Physics

Master's Thesis 2020:TIFX05
Department of Physics
Division of Subatomic, High Energy and Plasma Physics
Dark Matter Research Group
Chalmers University of Technology
SE-412 96 Gothenburg
Telephone +46 31 772 1000

Cover: Smallest detectable coupling constants corresponding to various dark matter particle masses in the XENONnT experiment under the assumption of a selection of dark matter-electron interactions. For more details, see Figure 6.2a.

Typeset in LaTeX
Printed by Chalmers Reproservice
Gothenburg, Sweden 2020

Prospects for the Discovery of General Dark Matter-Induced Atomic Responses
Finding the Statistical Significance for Signal Discovery of Future Experiments
OSKAR LINDROOS
Department of Physics
Chalmers University of Technology

Abstract

One of the major mysteries of modern physics is dark matter. Proposed by Fritz Zwicky in 1933, dark matter stands as the answer to several astronomical observations, but its constituents remain unkown. Since current observations only show dark matter interacting gravitationally, one can assume that the dark matter particle is a massive, weakly interacting particle also referred to as a WIMP. In an attempt to find the dark matter particle, large underground detectors have been constructed. These detectors utilise the principle of direct detection in order to detect weakly interacting particles. As the Earth passes through the halo of dark matter within the Milky Way one expects the flux of dark matter particles that arises to produce a signal within these experiments. However, so far a signal that cannot be anything other than dark matter remains to be found. This thesis will present the sensitivities for future direct detection experiments under the assumption of general dark matter-electron interactions. We provide the underlying theory of a model describing general dark matter-electron interactions in the non-relativistic frame which we use to simulate event rates in active experiments. Based on the null results in current experiments, we perform a statistical analysis in order to find the lowest detectable coupling constant for different sets of interactions corresponding to a specific dark matter particle mass. We express the sensitivity of future direct detection experiments in terms of statistical significance for signal discovery.

Keywords: dark matter, direct detection, statistical significance, projected sensitivity.

Acknowledgements

I want to express my gratitude towards my supervisor Riccardo Catena for giving me the opportunity to work with him on this thesis. He has been a continuous source of knowledge and advice and has always been willing to help with problems or provide sources for any piece of information I would need. I would also like to thank Timon Emken for showing me how to use the code package that I extended upon as well as all the help he has provided me with in regards to debugging and improving code efficiency.

Last, but not least, I would like to thank the research group as a whole. The company and interesting discussions during lunches, coffee breaks and evenings has made me feel more than welcome and has made this time so much more enjoyable.

Oskar Lindroos, Gothenburg, June 2020

Contents

List of Figures

List of Tables

1
Introduction

Current observations suggest that the majority of the matter in the universe is non-baryonic [1]. This non-baryonic matter is believed to exist due to its gravitational interaction on astronomical and cosmological scales. This as of yet unidentified form of matter has come to be called dark matter. The current paradigm suggests that dark matter may, apart from gravitationally, interact weakly with known particles.

Theories suggest that dark matter is distributed in a halo throughout the Milky Way. As the Earth moves through this halo, dark matter particles must also pass through the Earth. This motivates the so-called dark matter direct detection method. Direct detector experiments search for dark matter-electron or dark matter-nucleus interactions in deep underground detectors. If this scattering process would occur inside a detector, the energy transfer from the dark matter particle to the detector could be detectable.

However, the current null result in these searches constitutes a challenge for modern detectors. So far, these searches have only been able to probe certain cross section and dark matter particle mass ranges. For example, operating detectors based on dual phase argon and xenon targets has restricted dark matter candidates of mass larger than the proton mass and interacting with nucleons with cross sections at the weak scale. However, it is possible that the dark matter particle is found outside of the ranges currently being scanned. In particular, it could be lighter than a proton. In this case, the search for dark matter via electron recoils in argon and xenon detectors has been shown the be a promising venue to explore [2].

In an article produced by Catena et. al. the authors present a framework for general interactions between dark matter particles and electrons bound to atoms [3]. Compared to previous works, this general model allows for a wide range of possibilities through which dark matter can interact with electrons. However, an in-depth study of how this model will produce detectable signals in next-generation detectors is yet to be done.

1.1 Aim and purpose

The purpose of this thesis is to present the smallest detectable coupling constant for a given dark matter particle mass under various kinds of dark matter-electron interactions in direct detection experiments. These results can in turn be used when

designing next-generation direct detection experiments searching for dark matter in the Milky Way, such that the sensitivity will be high enough to probe dark matter under general interactions with electrons.

1.2 Method and thesis outline

In order to become familiar with the subject of dark matter and interactions between dark matter and nuclei as well as electrons, literature studies were made. This led into the main calculations of the thesis. These included deriving expressions that could be used to simulate an event rate in a detector, a scattering amplitude for a specific interaction type as well as adapting statistical hypothesis testing to the framework of this thesis. Following the analytical calculations was the numerical implementation. This began with becoming familiar with an existing code package used for producing results in a previous article [3]. The code package was then extended upon by introducing numerical simulations for hypothesis testing, as well as to compute the associated statistical significance for signal discovery. The extended code package could then be used to predict the sensitivity of next-generation experiments that searches for dark matter signals through scattering with electrons.

In Chapter 2 we begin by giving the reader a brief background on the field of dark matter physics including a summary of a few important milestones in the history of dark matter as well as its current state. We introduce a few experiments that are of interest as well as describe the fundamentals of their operating principles.

Chapter 3 focuses on the analytical calculations performed. We take a closer look at the details of deriving general dark matter-electron interactions. We show that this type of framework adds more degrees of freedom than previous works. We also show the necessity of such a framework by calculating the scattering amplitude for a specific model. We then consider the case in which an incoming dark matter particle scatters with an electron bound to an atom by introducing the dependence of the electron quantum state. We use this in order to find the differential rate at which dark matter ionises an atom target and relate this to the atomic response functions.

The statistical framework is presented in Chapter 4. Here we summarise methods of hypothesis testing using test statistics with data produced from Monte Carlo simulations. We also present how this can be adapted into testing theories in physics.

Chapter 5 gives the reader a detailed summary of how the numerical implementation is done. We show how the code package used in [3], which utilises the calculated atomic response functions using DarkARC [4], can be used to produce a signal, which we then use to perform the statistical simulations. We also describe how the hypothesis testing is implemented numerically. At the end we also specify the parameters that are of interest when producing results.

Chapter 6 presents the results of performing hypothesis testing using the parameters of the future direct detection experiment XENONnT. We show figures presenting

the projected sensitivity for this experiment for various dark matter-electron interaction operators. We also present how the sensitivity would change if XENONnT would scan more channels for the electron recoil energy.

Chapter 7 provides a discussion on the results presented. We also discuss the assumptions made as well as the limitations introduced. The chapter also discusses how this thesis can be improved upon as well as presenting ideas for future studies.

1.3 Limitations

This thesis will consider general interactions between dark matter particles and electrons. Even though this means a wider theory is studied, the work will still be limited to that of dark matter-electron interactions. The series of interactions will be truncated, meaning we will neglect high order interactions. The thesis will not consider nuclear recoils caused by dark matter. We also work in the non-relativistic limit. Furthermore, we will only consider dark matter interactions with xenon targets. In addition, we only consider the dark matter particle ionising the outermost electron of the electron shells.

2
Background

This chapter presents a brief background on the history of dark matter, highlighting a few milestones in the history of physics that has led scientists to search for the elusive source of several astronomical observations. We also give a summary on how experiments search for dark matter in modern times.

2.1 A historical summary

Dark matter is one of the major unsolved mysteries of modern physics. Many scientists agree that dark matter explains a number of astronomical observations, some of them reviewed below, but apart from observational evidence dark matter remains a mystery. The idea of dark matter, however, has not always been as well defined as it is today. It is an idea that has been under active development for decades, with many milestones along the way.

As early as in ancient Greece, the idea formed that there is more to this world than can be seen with the eye. The natural philosophers Leucippus and Democritus proposed the idea of the atom, the most fundamental building block of nature [1]. The atom was indivisible, and so small that it cannot be seen by the naked eye, yet they were infinite in number.

In 1687 Isaac Newton famously published *Philosophiæ Naturalis Principia Mathematica* in which he proposed his theory of gravity. This was revolutionary in the sense that scientists, for the first time, were able to explain and predict motions of stellar objects. Using Newton's theory of gravity, scientists were able to predict the existence of completely undiscovered astronomical objects. The mathematician Friederich Bessel predicted in 1844 the existence of faint companion stars, which explained the motions of the stars Sirius and Procyon [5]. Two years later, the astronomers Urbain Le Verrier and John Couch Adams used the theory of gravity to explain the anomalous motion of Uranus. They came to the conclusion that another planet had to exist beyond Uranus. Based on Le Verrier's precise calculations, astronomer John Galle was able to observe the new planet Neptune.

Lord Kelvin presented in a lecture in 1884 a method that would make it possible to approximate the masses of dark bodies in the Milky Way. By viewing the stars in the galaxy as a gas of particles interacting gravitationally he was able to find the amount of stars that would be needed in order to produce the observed velocity

dispersion of the stars in orbit around the galactical centre [6]. When the predicted number of stars did not match the observed, he proposed that the missing stars may be dark bodies.

Albert Einstein perfected the theory of gravity by proposing his general theory of relativity. Not only did he introduce a new view of the world, his theory also explained irregularities that had arisen in Newton's theory of gravity. The general theory of relativity also stated that gravity has an effect on light. Massive bodies can bend light if it enters a region of space time curved by the body. The massive bodies can also cause the wavelenght of light to change, leading to a redshift.

Astronomer Fritz Zwicky studied the redshifts of various galaxy clusters. In 1933 he noticed that the differences in velocity dispersions of the Coma Cluster exhibited differences of over 2000km/s [7]. This had already been discovered by Hubble and Humason, who were the ones that published the data that Zwicky studied. However, Zwicky would be the first to apply the virial theorem in order to estimate the mass of the cluster. His results showed that the observed mass of the Coma Cluster was far less than the mass that would cause the large velocity dipersions. He concluded that the majority of the mass in the cluster must be made up of some form of dark matter.

Needless to say, the idea of studying invisible objects is nothing new, and dark matter has for a long time been present in observations but its constituents remains to be detected. A prominent effect caused by dark matter is the shape of so called galactical rotation curves. Such curves show the rotational velocity of stars as a function of the radius from the galactical centre. Without dark matter, one would expect these functions to approach zero at larger radii. But instead, the velocity increases with the radius up to a certain point at which the velocity becomes near constant for increasing radius. This indicates a higher mass density in the outermost regions of the galaxy which is not accounted for by the baryonic mass.

Studies of gravitational lensing has proven to be closely related to dark matter. Observations of the so called Bullet Cluster has revealed that the mass distribution of the cluster does not align with the distribution of baryons. Instead, there has to be another gravitational source that shapes the cluster. Dark matter is believed to be this additional source of gravitational pull.

Studies of the Cosmic Microwave Background has proven to be effective when it comes to determining the density of baryons in the universe. The fluctuations in the CMB are inconsistent with a universe that is made up by only baryonic matter. Furthermore, by comparing the mass density to the baryonic density, one finds that in fact the majority of the universe is non-baryonic.

2.2 The standard halo model

The most common model for the distribution of dark matter within the Milky Way is called the standard halo model [8]. This model suggests that the dark matter

within the Milky Way forms a halo that extends far beyond the stellar disk. As the Earth passes through the halo, a flux of dark matter is generated. This flux depends on the velocity distribution for the dark matter particles. The standard halo model describes this velocity distribution as a Maxwellian distribution

$$f_\chi(\mathbf{v}) = \frac{1}{N_{\text{esc}}\pi^{3/2}v_0^3}\exp\left[-\frac{(\mathbf{v}+\mathbf{v}_\oplus)^2}{v_0^2}\right]\Theta(v_{\text{esc}} - |\mathbf{v}+\mathbf{v}_\oplus|) \tag{2.1}$$

where the normalisation constant N_{esc} is

$$N_{\text{esc}} = \text{erf}(v_{\text{esc}}/v_0) - \frac{2}{\sqrt{\pi}}\frac{v_{\text{esc}}}{v_0}\exp\left(-\frac{v_{\text{esc}}^2}{v_0^2}\right). \tag{2.2}$$

Here, $v_\oplus = 244$ km/s denotes the velocity of the Earth, $v_0 = 220$ km/s is the root-mean square velocity dispersion and $v_{\text{esc}} = 544$km/s is the upper bound for the dark matter particle velocities. If the velocity of the dark matter particle exceeds v_{esc} it will escape the gravitational pull. The halo is considered isotropic with a local density of $\rho_\chi = 0.4$ GeV/cm^3 where the dark matter density is given by the number density multiplied by the dark matter particle mass $\rho_\chi = n_\chi m_\chi$.

2.3 Direct detection

One of the most promising methods for detecting dark matter is direct detection. These experiments utilise large underground tanks filled with noble gas in both liquid and gas form. The idea behind these experiments is that as the Earth passes through the dark matter halo, some particles will pass through the detector. Given that the dark matter particle can interact with the detector and ionise an atom within, the electron can be picked up by the detector and produce a signal.

Current observations tell us that dark matter interacts gravitationally, but other types of interactions are not experimentally excluded. For example, weak scale interactions between dark matter and electrons are compatible with the null result of operating direct detection experiments. Dark matter particles of this type are often referred to as weakly interacting massive particles, or WIMPs, and are one of the most promising candidates for the dark matter particle [9]. When searching for WIMPs, direct detection experiments appear most promising. Being placed deep underground, the detectors become shielded from most background signals such as cosmic rays.

As mentioned, these kinds of experiments utilise noble gases as the target material, in both liquid and gaseous form. The most common targets in use are argon and xenon. Argon is used as a target in experiments such as the DarkSide-50 detector [10]. The XENON collaboration focuses instead on xenon targets. Their latest experiment XENON1T recently concluded the data collection. This data has been analysed to set new exclusion limits for the possible dark matter particle mass and the corresponding interaction strength [11]. The XENON collaboration is also upgrading their detector into a larger one with higher sensitivity, called the XENONnT.

The interpretation of direct detection experiments rely heavily on the type of interaction. These kinds of experiments can be used if the dark matter particle interacts with either nuclei or electrons. The dark matter-electron interaction models studied so far has been restrictive, depending only on the momentum transfer in the scattering process. Recently, however, a paper was published by Catena et. al. [3] in which the authors use effective theory methods to present a new model for dark matter-electron interactions. The model describes general interactions and allows for more ways in which the dark matter particle can scatter with the electron. This opens up a wide range of possible signals that has not earlier been considered in experiments.

3

Theory

This chapter introduces the theoretical framework that is simulated numerically in later chapters. We present a thorough derivation of the model for dark matter-electron interactions that is presented in [3]. We begin by deriving the kinematics of the model, which implements the fundamentals of energy and momentum conservation. Afterwards, we present the quantum mechanical calculations for extracting a transition rate. This rate is then evaluated using a scattering amplitude for general dark matter-electron interactions. The general framework is then taken to the specific case of ionisation of atoms. All calculations are performed in natural units, where $c = \hbar = 1$.

3.1 Kinematics

Before investigating the quantum mechanical aspects of dark matter-electron scattering, it is important that one understands the underlying kinematics. In this section we assume that the dark matter particle is the incoming particle and that the electron is bound to an atom. The principle we study is energy conservation, since momentum is not conserved in the dark matter scattering by bound electrons.

As for an initial state of the system, we take the dark matter particle with mass m_χ carrying a momentum $\mathbf{p}$ to be travelling towards an electron of mass m_e carrying a momentum $\mathbf{k}$. The electron is bound to an atom with a binding energy E_1. When the two scatter, the dark matter particle transfers the momentum $\mathbf{q}$ to the electron. This causes a change in momentum for both particles such that $\mathbf{p} \to \mathbf{p}'$ and $\mathbf{k} \to \mathbf{k}'$. Furthermore, the kinetic energy of the dark matter particle T_χ may induce a change in energy for the electron. This would mean that as $T_\chi \to T'_\chi$ we get $E_1 \to E_2$. Before and after scattering the system has the total energies E_i and E_f respectively. The scattering process is described by Figure 3.1.

The momenta of the system are denoted such that the momentum for the electron before and after scattering are $\mathbf{k}$ and $\mathbf{k}'$. For the dark matter particle, the momentum before and after scattering are denoted $\mathbf{p}$ and $\mathbf{p}'$. As seen in Figure 3.1, the momentum transfer $\mathbf{q}$ is the momentum transferred from the dark matter particle to the electron. This means that

$$\mathbf{q} = \mathbf{p} - \mathbf{p}' = \mathbf{k}' - \mathbf{k}. \tag{3.1}$$

The initial kinetic energy T_χ is written classically as $T_\chi = \frac{1}{2} m_\chi v^2$, where $v = |\mathbf{p}|/m_\chi$,

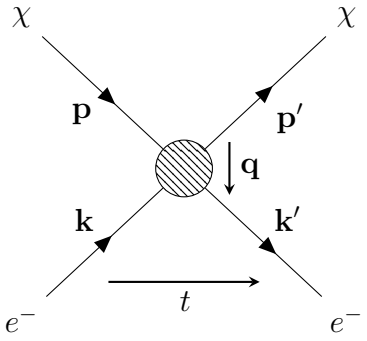

(a) Diagram showing the momenta in the system.

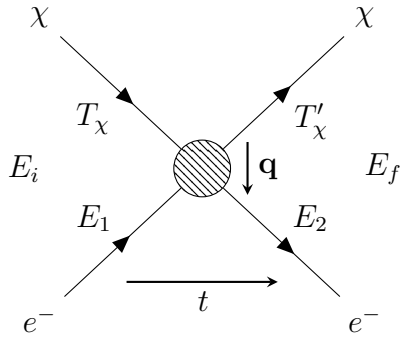

(b) Diagram showing the energies in the system.

Figure 3.1: Diagrams showing the kinematics of a dark matter particle scattering with an electron. Figure 3.1a shows the incoming and outgoing momenta of the scattering, as well as the momentum transfer vector **q**. Figure 3.1b shows the energies at the different stages of the scattering. The energy shown for the dark matter particle is kinetic, while the energy shown for the electron is the binding energy before and after scattering. E_i and E_f are the total initial and final energies of the system. The direction of time is indicated by t.

and the final kinetic energy as $T'_\chi = \frac{1}{2m_\chi}|\mathbf{p}'|^2$. From (3.1) it follows that

$$T'_\chi = \frac{1}{2}m_\chi v^2 + \frac{1}{2m_\chi}q^2 - vq\cos\theta_{vq} \tag{3.2}$$

where the final term arises from $\mathbf{v}\cdot\mathbf{q} = vq\cos\theta_{vq}$. With the rest mass energies being m_e and m_χ for the electron and dark matter particle respectively, we are able to write the total energies before and after scattering as

$$E_i = m_\chi + m_e + \frac{1}{2}m_\chi v^2 + E_1, \tag{3.3}$$

$$E_f = m_\chi + m_e + \frac{1}{2}m_\chi v^2 + \frac{1}{2m_\chi}q^2 - vq\cos\theta_{vq} + E_2. \tag{3.4}$$

As stated above, E_1 and E_2 are the binding energies for the electron before and after scattering. The total difference in energy can thus be written as

$$E_f - E_i = \Delta E_{1\to 2} + \frac{1}{2m_\chi}q^2 - vq\cos\theta_{vq} \tag{3.5}$$

where $\Delta E_{1\to 2} = E_2 - E_1$. In the scattering of dark matter particles by bound electrons, energy is conserved, i.e. $E_f - E_i = 0$.

3.2 Finding the total transition rate

The total transition rate for the scattering event, a probabilistic process, depends on the nature of the interaction as well as the structure of the system. In quantum field

theory, this probability is described by a scattering amplitude, $\mathcal{M}$. In this section, we will relate this scattering amplitude to the total transition rate.

In order to find the scattering amplitude for a given event, we will relate the amplitude to the elements of the S-matrix. We may expand the S-matrix in a Dyson series as

$$S = \sum_{n=0}^{\infty} \frac{(-i)^n}{n!} \int ... \int \mathrm{d}^4x_1 ... \mathrm{d}^4x_n \mathrm{T}\left[H_I(x_1)...H_I(x_n)\right] \tag{3.6}$$

where T denotes time ordering and H_I is the interaction Hamiltonian. If we denote the initial state of the system by $|i\rangle$, and the final state by $|f\rangle$, the first term in this expansion corresponds to

$$S_{\mathrm{fi}} = -i \int \mathrm{d}^4x \, \langle f| \, H_I \, |i\rangle \, . \tag{3.7}$$

This expression can be rewritten in terms of the initial and final electron wave functions,

$$S_{\mathrm{fi}} = -2\pi i \delta(E_f - E_i) \int \mathrm{d}^3x \int \int \frac{\mathrm{d}^3k}{(2\pi)^3} \frac{\mathrm{d}^3k'}{(2\pi)^3} \, \langle e_2|\mathbf{k}'\rangle \, \langle \mathbf{k}', \mathbf{p}'| \, H_S \, |\mathbf{p}, \mathbf{k}\rangle \, \langle \mathbf{k}|e_1\rangle \, . \tag{3.8}$$

Here we have gone from the interaction picture Hamiltonian to the Schrödinger picture Hamiltonian H_S with E_i and E_f representing the total initial and final energy of the system. Also, we have expanded the initial and final states such that $|i\rangle = |e_1, \mathbf{p}_i\rangle$ and $|f\rangle = |e_2, \mathbf{p}'\rangle$ where e_1 and e_2 are the energy eigenvalues for the electron. The momenta $\mathbf{k}$ and $\mathbf{k}'$ are the initial and final momenta for the electron while $\mathbf{p}$ and $\mathbf{p}'$ are the initial and final momenta for the dark matter particle. The momentum states are normalised such that

$$\int \frac{\mathrm{d}^3k}{(2\pi)^3} \, |\mathbf{k}\rangle \, \langle \mathbf{k}| = \mathbb{1}, \tag{3.9}$$

and

$$\langle \mathbf{p}|\mathbf{p}\rangle = \int \mathrm{d}^3x \; e^{i(\mathbf{p}-\mathbf{p})x} = (2\pi)^3 \delta^{(3)}(0) = V. \tag{3.10}$$

In the case of scattering against a free electron $|\mathbf{k}, \mathbf{p}\rangle \to |\mathbf{k}', \mathbf{p}'\rangle$ we simply have the matrix element

$$S_{\mathrm{fi}}^{\mathrm{free}} = -2\pi i \delta(\widetilde{E_f} - \widetilde{E_i}) \int \mathrm{d}^3x \, \langle \mathbf{p}', \mathbf{k}'| \, H_S \, |\mathbf{k}, \mathbf{p}\rangle \tag{3.11}$$

where $\widetilde{E_i}$ and $\widetilde{E_f}$ are the total initial and final energies for this case. The matrix element for scattering against a free electron is related to the scattering amplitude $\mathcal{M}$ as

$$S_{\mathrm{fi}}^{\mathrm{free}} = i(2\pi)^4 \delta(\widetilde{E_f} - \widetilde{E_i}) \delta^{(3)}(\mathbf{p}' + \mathbf{k}' - \mathbf{p} - \mathbf{k}) \frac{1}{\sqrt{2E_{\mathbf{k}} 2E_{\mathbf{k}'} 2E_{\mathbf{p}} 2E_{\mathbf{p}'}}} \mathcal{M}(\mathbf{k}, \mathbf{k}', \mathbf{p}, \mathbf{p}'), \tag{3.12}$$

where $E_{\mathbf{k}} = \sqrt{|\mathbf{k}|^2 + m_e^2}$ and $E_{\mathbf{p}} = \sqrt{|\mathbf{p}|^2 + m_\chi^2}$. By setting (3.11) and (3.12) equal, one may find that

$$\int \mathrm{d}^3x \, \langle \mathbf{p}', \mathbf{k}' | \, H_S \, | \mathbf{k}, \mathbf{p} \rangle = -(2\pi)^3 \delta^{(3)}(\mathbf{p}'+\mathbf{k}'-\mathbf{p}-\mathbf{k}) \frac{1}{\sqrt{2E_{\mathbf{k}} 2E_{\mathbf{k}'} 2E_{\mathbf{p}} 2E_{\mathbf{p}'}}} \mathcal{M}(\mathbf{k}, \mathbf{k}', \mathbf{p}, \mathbf{p}'). \tag{3.13}$$

This can be substituted into (3.8). After integrating over $\mathbf{k}'$ in the non-relativistic limit, the matrix element can be written as

$$S_{\mathrm{fi}} = 2\pi i \delta(E_f - E_i) \int \frac{\mathrm{d}^3k}{(2\pi)^3} \frac{\mathcal{M}(\mathbf{k}, \mathbf{p}, \mathbf{q})}{4 m_\chi m_e} V \psi_2^*(\mathbf{k}+\mathbf{q}) \psi_1(\mathbf{k}). \tag{3.14}$$

Here we have identified the momentum transfer (3.1) as well as the electron mass m_e and the dark matter particle mass m_χ. The electron wave functions have been rewritten as $\langle \mathbf{k} | e_1 \rangle = \frac{1}{\sqrt{V}} \psi_1(\mathbf{k})$ and $\langle e_2 | \mathbf{k} + \mathbf{q} \rangle = \frac{1}{\sqrt{V}} \psi_2^*(\mathbf{k}+\mathbf{q})$ where V is the volume element that determines the normalisation.

In order to find the total rate at which incoming dark matter particles ionise bound electrons we need to find the probability for such a transition. The probability for a transition of the dark matter particle state $|e_1, \mathbf{p}\rangle \to |e_2, \mathbf{p}'\rangle$ is given by the element $|S_{\mathrm{fi}}|^2/V^4$. For a transition from $\mathbf{p}'$ into $\mathbf{p}' + \mathrm{d}\mathbf{p}'$ we write the probability as

$$P(\mathbf{p}) = \frac{|S_{\mathrm{fi}}|^2}{V^4} \frac{V \mathrm{d}^3 p'}{(2\pi)^3} = \frac{|S_{\mathrm{fi}}|^2}{V^4} \frac{V \mathrm{d}^3 \mathrm{q}}{(2\pi)^3}. \tag{3.15}$$

The absolute value of the matrix element squared is simply obtained from (3.14) as

$$|S_{\mathrm{fi}}|^2 = |2\pi i \delta(E_f - E_i)|^2 \left| \int \frac{\mathrm{d}^3k}{(2\pi)^3} \frac{V}{4 m_\chi m_e} \psi_2^*(\mathbf{k}+\mathbf{q}) \mathcal{M}(\mathbf{k}, \mathbf{p}, \mathbf{q}) \psi_1(\mathbf{k}) \right|^2. \tag{3.16}$$

The term $|2\pi i \delta(E_f - E_i)|^2$ can be rewritten by applying the square as

$$|2\pi i \delta(E_f - E_i)|^2 = (2\pi \delta(E_f - E_i)) \, (2\pi \delta(E_f - E_i)) \, . \tag{3.17}$$

By applying the integral expression for one of the dirac delta functions

$$2\pi \delta(E_f - E_i) = \int \mathrm{d}t \; e^{i(E_f - E_i)t} \tag{3.18}$$

we can rewrite the original term $|2\pi i \delta(E_f - E_i)|^2$ such that

$$|2\pi i \delta(E_f - E_i)|^2 = 2\pi \delta(E_f - E_i) T \tag{3.19}$$

where T denotes the divergent integral over t that arises by setting $E_f = E_i$ in (3.18). Interestingly enough, both V and T are divergent factors that vanish in the final expression. Using this rewritten form of the delta function squared, we find that

$$\frac{|S_{\text{fi}}|^2}{V^4} = 2\pi\delta(E_f - E_i)\frac{T}{16m_\chi^2 m_e^2 V^2}\left|\int \frac{\mathrm{d}^3k}{(2\pi)^3}\psi_2^*(\mathbf{k}+\mathbf{q})\mathcal{M}(\mathbf{k},\mathbf{p},\mathbf{q})\psi_1(\mathbf{k})\right|^2. \quad (3.20)$$

The absolute value squared of the integral can be rewritten for simplicity as

$$|\mathcal{M}_{1\to 2}|^2 = \left|\int \frac{\mathrm{d}^3k}{(2\pi)^3}\psi_2^*(\mathbf{k}+\mathbf{q})\mathcal{M}(\mathbf{k},\mathbf{p},\mathbf{q})\psi_1(\mathbf{k})\right|^2. \quad (3.21)$$

This is what we will refer to as the squared transition amplitude. Thus we get the probability for the transition as

$$P(\mathbf{p}) = 2\pi\delta(E_f - E_i)\frac{T}{16m_\chi^2 m_e^2 V}\frac{\mathrm{d}^3\mathrm{q}}{(2\pi)^3}|\mathcal{M}_{1\to 2}|^2. \quad (3.22)$$

The transition rate for one dark matter particle is given by $P(\mathbf{p})V/T$. We weigh this factor with the initial dark matter particle velocity distribution (2.1) as well as the local dark matter number density. Integrating over the dark matter velocity as well as the momentum transfer gives the total transition rate

$$R_{1\to 2} = \int n_\chi f_\chi(\mathbf{v})\frac{P(\mathbf{p})V}{T}\mathrm{d}^3v, \quad (3.23)$$

or, by inserting the explicit expression for the transition probability (3.22),

$$R_{1\to 2} = (2\pi)\delta(E_f - E_i)\frac{n_\chi}{16m_\chi^2 m_e^2}\int \frac{\mathrm{d}^3q}{(2\pi)^3}\int \mathrm{d}^3v\ f_\chi(\mathbf{v})|\mathcal{M}_{1\to 2}|^2. \quad (3.24)$$

Note that the divergent factors T as well as the state normalisation factors V all vanish in the final expression. So (3.24) depends only on the number density n_χ , the dark matter velocity distribution f_χ, the masses m_χ and m_e, the initial and final state wave functions for the electron, the scattering amplitude $\mathcal{M}(\mathbf{k},\mathbf{p},\mathbf{q})$ and the initial and final energies E_i and E_f. Note also that $n_\chi = \rho_\chi/m_\chi$ where ρ_χ is the local dark matter density.

3.3 Finding the squared amplitude $|\mathcal{M}_{1\to 2}|^2$

The amplitude for dark matter scattering by free electrons can be written as

$$\mathcal{M}(\mathbf{k},\mathbf{k}',\mathbf{p},\mathbf{p}') = \mathcal{M}(\mathbf{v}_{\text{el}}^{\perp},\mathbf{q}). \quad (3.25)$$

This expression relies on the fact that momentum conservation and Galilean invariance allow us to express $\mathcal{M}$ as a function of two linear combinations of particle momenta $\mathbf{q}$ and $\mathbf{v}_{\text{el}}^{\perp} = \mathbf{v} - \mathbf{q}/2\mu - \mathbf{k}/m_e$ where μ is the reduced mass for the dark matter particle and the electron [12]. Galilean invariance corresponds to Lorentz invariance in the non-relativistic limit. In order to find a general theory, we need to write $\mathcal{M}(\mathbf{v}_{\text{el}}^{\perp},\mathbf{q})$ in the most general way possible. In accordance with the articles written by Dobrescu and Mocioiu [13] and Fan et. al. [14] there are four independent, Hermitian factors that determine the interactions, namely $\mathbf{v}_{\text{el}}^{\perp}, \mathbf{q}, \mathbf{S}_\chi$ and $\mathbf{S}_e$,

where $\mathbf{S}_e$ and $\mathbf{S}_\chi$ are the spin operators for the electron and dark matter particle. These can be combined in order to form an infinite set of interaction operators, but we choose to restrict ourselves to the leading terms. At linear order in $\mathbf{v}_{\text{el}}^\perp$ and second order in $\mathbf{q}$ it is possible to form 14 different combinations of these that are invariant under 3D rotations as well as Galilean transformations. These scalar operators and their numbering follow from [13] and [14] and are listed in Table 3.1.

$$
\begin{aligned}
&\mathcal{O}_1 = \mathbb{1}_\chi \mathbb{1}_e && \mathcal{O}_3 = i\mathbf{S}_e \cdot \left(\tfrac{\mathbf{q}}{m_e} \times \mathbf{v}_{\text{el}}^\perp\right) \\
&\mathcal{O}_4 = \mathbf{S}_\chi \cdot \mathbf{S}_e && \mathcal{O}_5 = i\mathbf{S}_\chi \cdot \left(\tfrac{\mathbf{q}}{m_e} \times \mathbf{v}_{\text{el}}^\perp\right) \\
&\mathcal{O}_6 = \left(\mathbf{S}_\chi \cdot \tfrac{\mathbf{q}}{m_e}\right)\left(\mathbf{S}_e \cdot \tfrac{\mathbf{q}}{m_e}\right) && \mathcal{O}_7 = \mathbf{S}_e \cdot \mathbf{v}_{\text{el}}^\perp \mathbb{1}_\chi \\
&\mathcal{O}_8 = \mathbf{S}_\chi \cdot \mathbf{v}_{\text{el}}^\perp \mathbb{1}_e && \mathcal{O}_9 = i\mathbf{S}_\chi \cdot \left(\mathbf{S}_e \times \tfrac{\mathbf{q}}{m_e}\right) \\
&\mathcal{O}_{10} = i\mathbf{S}_e \cdot \tfrac{\mathbf{q}}{m_e} \mathbb{1}_\chi && \mathcal{O}_{11} = i\mathbf{S}_\chi \cdot \tfrac{\mathbf{q}}{m_e} \mathbb{1}_e \\
&\mathcal{O}_{12} = \mathbf{S}_\chi \cdot \left(\mathbf{S}_e \times \mathbf{v}_{\text{el}}^\perp\right) && \mathcal{O}_{13} = i\left(\mathbf{S}_\chi \cdot \mathbf{v}_{\text{el}}^\perp\right)\left(\mathbf{S}_e \cdot \tfrac{\mathbf{q}}{m_e}\right) \\
&\mathcal{O}_{14} = i\left(\mathbf{S}_e \cdot \mathbf{v}_{\text{el}}^\perp\right)\left(\mathbf{S}_\chi \cdot \tfrac{\mathbf{q}}{m_e}\right) && \mathcal{O}_{15} = i\mathcal{O}_{11}\left[\left(\mathbf{S}_e \times \mathbf{v}_{\text{el}}^\perp\right) \cdot \tfrac{\mathbf{q}}{m_e}\right]
\end{aligned}
$$

Table 3.1: A list over the different operators that can be formed from $\mathbf{v}_{\text{el}}^\perp, \mathbf{q}, \mathbf{S}_\chi$ and $\mathbf{S}_e$ while being at most linear in $\mathbf{v}_{\text{el}}^\perp$ and second order in $\mathbf{q}$. The operator $\mathcal{O}_2$ is of second order in $\mathbf{v}_{\text{el}}^\perp$ and has thus been excluded. The list of operators presented is based on the theory presented in the articles written by Dobrescu and Mocioiu [13] and Fan et. al. [14].

These operators are at most first order in $\mathbf{v}_{\text{el}}^\perp$ and second order in $\mathbf{q}$. Using these operators, we can write a general form for the scattering amplitude such that

$$
\mathcal{M}(\mathbf{v}_{\text{el}}^\perp, \mathbf{q}) = \sum_i \left(c_i^s + c_i^l \frac{q_{\text{ref}}^2}{|\mathbf{q}|^2}\right) \langle \mathcal{O}_i \rangle \,. \tag{3.26}
$$

The coefficients c_i^s and c_i^l corresponds to the coupling constants for short-range- and long-range interactions respectively, with s denoting short-range and l denoting long-range. Short-range interaction denotes the type of interaction where the mass of the mediator particle is much larger than the momentum transfer, and long-range interaction indicates that the mass of the mediator particle is small, or close to zero. Angle brackets in (3.26) denote a multiplication by two-component spinors. For operator $\mathcal{O}_1$ this would be $\langle \mathcal{O}_1 \rangle = \xi_\chi^\dagger \mathbb{1} \xi_\chi \xi_e^\dagger \mathbb{1} \xi_e$, where ξ_χ and ξ_e are two-component spinors for the dark matter and electron respectively. The reference momentum is $q_{\text{ref}} = \alpha m_e$ where $\alpha = 1/137$.

If one assumes the scattering amplitude (3.26), one may expand the free electron scattering amplitude as

$$
\mathcal{M}(\mathbf{v}_{\text{el}}^\perp, \mathbf{q}) = \mathcal{M}(\mathbf{v}_{\text{el}}^\perp, \mathbf{q})_{\mathbf{k}=0} + \left(\frac{\mathbf{k}}{m_e}\right) \cdot m_e \nabla_{\mathbf{k}} \mathcal{M}(\mathbf{v}_{\text{el}}^\perp, \mathbf{q})_{\mathbf{k}=0}. \tag{3.27}
$$

Since the amplitude is at most linear in $\mathbf{v}_{\text{el}}^\perp$ there will be no further terms in the expansion, and (3.27) is the exact expression. If one substitutes the general amplitude (3.25) into the transition amplitude (3.21) we get

$$|\mathcal{M}_{1\to 2}|^2 = \left| \int \frac{\mathrm{d}^3k}{(2\pi)^3} \psi_2^*(\mathbf{k}+\mathbf{q}) \mathcal{M}(\mathbf{v}_{\mathrm{el}}^{\perp}, \mathbf{q}) \psi_1(\mathbf{k}) \right|^2 . \tag{3.28}$$

Applying the expansion in (3.27) gives

$$|\mathcal{M}_{1\to 2}|^2 = \left| \int \frac{\mathrm{d}^3k}{(2\pi)^3} \psi_2^*(\mathbf{k}+\mathbf{q}) \left[\mathcal{M}(\mathbf{v}_{\mathrm{el}}^{\perp}, \mathbf{q}) + \left(\frac{\mathbf{k}}{m_e} \right) \cdot m_e \nabla_{\mathbf{k}} \mathcal{M}(\mathbf{v}_{\mathrm{el}}^{\perp}, \mathbf{q}) \right] \psi_1(\mathbf{k}) \right|^2_{\mathbf{k}=0} . \tag{3.29}$$

By evaluating the square one finds the transition amplitude squared as

$$\begin{aligned} |\mathcal{M}_{1\to 2}|^2 = \Bigg\{ & \left| \mathcal{M}(\mathbf{v}_{\mathrm{el}}^{\perp}, \mathbf{q}) \right|^2 |f_{1\to 2}(\mathbf{q})|^2 + m_e^2 \left| \nabla_{\mathbf{k}} \mathcal{M}(\mathbf{v}_{\mathrm{el}}^{\perp}, \mathbf{q}) \cdot \mathbf{f}_{1\to 2}(\mathbf{q}) \right|^2 \\ & + 2 m_e \mathcal{R} \left[\mathcal{M}(\mathbf{v}_{\mathrm{el}}^{\perp}, \mathbf{q}) f_{1\to 2}(\mathbf{q}) \nabla_{\mathbf{k}} \mathcal{M}(\mathbf{v}_{\mathrm{el}}^{\perp}, \mathbf{q}) \cdot \mathbf{f}_{1\to 2}^*(\mathbf{q}) \right] \Bigg\}_{\mathbf{k}=0} , \end{aligned} \tag{3.30}$$

where we take the real part of the third term. In this expression we have identified two atomic form factors. These depend on properties of the atom. The first one we find is the scalar atomic form factor

$$f_{1\to 2}(\mathbf{q}) = \int \frac{\mathrm{d}^3k}{(2\pi)^3} \psi_2^*(\mathbf{k}+\mathbf{q}) \psi_1(\mathbf{k}). \tag{3.31}$$

Comparing the scalar atomic form factor with (3.21) it becomes apparent that (3.31) allows for a simple way to access the transition amplitude from the free electron scattering amplitude through

$$\mathcal{M}_{1\to 2}(\mathbf{q}) = \mathcal{M}(\mathbf{q}) \times f_{1\to 2}(\mathbf{q}). \tag{3.32}$$

The second form factor we find is the vectorial atomic form factor

$$\mathbf{f}_{1\to 2}(\mathbf{q}) = \int \frac{\mathrm{d}^3k}{(2\pi)^3} \psi_2^*(\mathbf{k}+\mathbf{q}) \left(\frac{\mathbf{k}}{m_e} \right) \psi_1(\mathbf{k}). \tag{3.33}$$

While the scalar atomic form factor (3.31) is well known and has been previously studied, the vectorial atomic form factor (3.33) is new and was first discovered by Catena et. al. [3]. The fact that we get the additional vectorial form factor is due to the approach leading to the general scattering amplitude (3.26). This means that the transition amplitude (3.30) incorporates both the free electron scattering amplitude as well as properties of the atom. Thus this becomes the more general form of (3.21).

3.4 Validity of the approach $\mathcal{M}(\mathbf{v}_{\mathrm{el}}^{\perp}, \mathbf{q})$, the anapole

Previous works have considered the case of $\mathcal{M}(\mathbf{q})$, i.e. scattering amplitudes that do not depend on $\mathbf{v}_{\mathrm{el}}^{\perp}$. However this only contributes to the first term in (3.30). The rest of the squared transition amplitude gives rise to results depending on $\mathbf{v}_{\mathrm{el}}^{\perp}$ in the

scattering amplitude. In this section we perform a calculation that shows that our realisation of $\mathcal{M}$ is well motivated. Focusing on the anapole dark matter model, we will find a scattering amplitude that depends on both $\mathbf{v}_{\text{el}}^{\perp}$ and $\mathbf{q}$ explicitly. We follow the calculations of previous works by Nobile et. al. [15] as well as Catena et. al. [16].

Consider the interaction Lagrangian for the anapole interaction

$$\mathcal{L} = \frac{1}{2}\frac{g}{\Lambda^2}\bar{\chi}\gamma^{\mu}\gamma^5\chi\partial^{\nu}F_{\mu\nu}. \tag{3.34}$$

Here, χ is the dark matter particle as a Majorana fermion, g is a dimensionless coupling constant for the interaction, Λ is a mass scale, γ^{μ} along with γ^5 are the gamma matrices and $F_{\mu\nu}$ is the Maxwell tensor. Through a manipulation of the indices and by expanding the Maxwell tensor as $F_{\mu\nu} = \partial_{\mu}A_{\nu} - \partial_{\nu}A_{\mu}$, one can rewrite (3.34) as

$$\mathcal{L} = \frac{1}{2}\frac{g}{\Lambda^2}\bar{\chi}\gamma_{\lambda}\gamma^5\chi\left(\partial^{\mu}\partial^{\lambda} - g^{\mu\lambda}\partial^{\nu}\partial_{\nu}\right)A_{\mu} \tag{3.35}$$

where $g^{\mu\lambda}$ is the flat spacetime metric. Through partial integration, ignoring boundary terms, the Lagrangian becomes

$$\mathcal{L} = \frac{1}{2}\frac{g}{\Lambda^2}\left(\partial^{\mu}\partial^{\lambda} - g^{\mu\lambda}\partial^{\nu}\partial_{\nu}\right)\left[\bar{\chi}\gamma_{\lambda}\gamma^5\chi\right]A_{\mu}, \tag{3.36}$$

such that the derivatives act on $\bar{\chi}\gamma_{\lambda}\gamma^5\chi$ rather than A_{μ}. Identifying the interaction current

$$j^{\mu} = -\frac{1}{2}\frac{g}{\Lambda^2}\left(g^{\mu\lambda}\partial^{\nu}\partial_{\nu} - \partial^{\mu}\partial^{\lambda}\right)\bar{\chi}\gamma_{\lambda}\gamma^5\chi \tag{3.37}$$

allows us to write the Lagrangian in its simplest form

$$\mathcal{L} = -j^{\mu}A_{\mu}. \tag{3.38}$$

The interaction Lagrangian is related to the S-matrix such that

$$S = i\int \mathrm{d}^4x \,\langle \mathbf{p}', \mathbf{k}', s', r'|\, \mathcal{L}(x)\, |\mathbf{p}, \mathbf{k}, s, r\rangle \tag{3.39}$$

where $\mathbf{p}$ and $\mathbf{k}$ are the initial momenta for the dark matter particle and electron, $\mathbf{p}'$ and $\mathbf{k}'$ are the corresponding final momenta, s and r are the initial spins for the dark matter particle and electron and s' and r' are the final spins. By inserting the Lagrangian in (3.38) into (3.39) and performing a propagation of the current, one may write the S-matrix as

$$S = -i\,\langle \mathbf{p}', s'|\, j^{\mu}(0)\, |\mathbf{p}, s\rangle\, \langle \mathbf{k}', r'|\, A_{\mu}(q)\, |\mathbf{k}, r\rangle\,, \tag{3.40}$$

where $A_{\mu}(q)$ is the Fourier transformation of $A_{\mu}(x)$ and q is the four-momentum transfer. The two terms in this expression can now be evaluated separately. The first term can be evaluated by using the properties of Majorana spinors. We may expand these spinors in a set of annihilation and creation operators, $a_{\mathbf{p}}^{s}$ and $a_{\mathbf{p}}^{s\dagger}$, as well as four-component spinors $u^s(p)$. This expansion is given in Peskin and Schroeder [17] and reads

$$\chi(x) = \int \frac{\mathrm{d}^3 p}{(2\pi)^3} \frac{1}{\sqrt{2E_{\mathbf{p}}}} \sum_s \left(a^s_{\mathbf{p}} u^s(p) e^{-ip\cdot x} + a^{s\dagger}_{\mathbf{p}} u^{s*}(p) e^{ip\cdot x} \right), \tag{3.41}$$

where $E_{\mathbf{p}} = \sqrt{|\mathbf{p}|^2 + m_\chi^2}$. Inserting the field expansion (3.41) into (3.37) along with the definition $\bar{\chi} = \chi^\dagger \gamma^0$ as well as using the anticommutator rule $\{a^{s'}_{\mathbf{p}'}, a^s_{\mathbf{p}}\} = (2\pi)^3 \delta^{(3)}(\mathbf{p} - \mathbf{p}') \delta^{ss'}$ it is possible to find that

$$\langle \mathbf{p}', s' | \, j^\mu(0) \, | \mathbf{p}, s \rangle = \frac{1}{\sqrt{2E_{\mathbf{p}} 2E_{\mathbf{p}'}}} \frac{g}{\Lambda^2} \left(q^2 g^{\mu\lambda} - q^\mu q^\lambda \right) \bar{u}^{s'}(p') \gamma_\lambda \gamma^5 u^s(p). \tag{3.42}$$

For the second term in (3.40), we use the Maxwell equations $\partial_\mu F^{\mu\nu} = eJ^\nu$ along with a translation of the current to write

$$\langle \mathbf{k}', r' | \, A_\mu(q) \, | \mathbf{k}, r \rangle = -(2\pi)^4 \delta^{(4)}(p' + k' - p - k) \frac{e}{q^2} \langle \mathbf{k}', r' | \, J_\mu(0) \, | \mathbf{k}, r \rangle, \tag{3.43}$$

where p, k, p' and k' are four-vectors. The matrix element for the four-current J_μ may in turn be rewritten in terms of electromagnetic form factors F_1 and F_2

$$\langle \mathbf{k}', r' | \, J_\mu(0) \, | \mathbf{k}, r \rangle = \frac{1}{\sqrt{2E_{\mathbf{k}} 2E_{\mathbf{k}'}}} \bar{v}^{r'}(k') \left[F_1(q^2) \gamma_\mu + \frac{i}{2m_e} F_2(q^2) \sigma_{\mu\nu} q^\nu \right] v^r(k). \tag{3.44}$$

Here, $v^r(k)$ is the four-component spinor of the electron, and $\sigma^{\mu\nu} = \frac{i}{2}[\gamma^\mu, \gamma^\nu]$. In order to find the scattering amplitude $\mathcal{M}$ for the anapole interaction we need to relate it to the S-matrix element (3.39). The two are related as

$$S = \frac{1}{\sqrt{2E_{\mathbf{p}} 2E_{\mathbf{p}'} 2E_{\mathbf{k}} 2E_{\mathbf{k}'}}} (2\pi)^4 \delta^{(4)}(p' + k' - p - k) i\mathcal{M} \tag{3.45}$$

By setting (3.40) and (3.45) equal, and substituting the expressions for the matrix elements (3.42) and (3.43), one finds that the scattering amplitude $\mathcal{M}$ is

$$\mathcal{M} = \frac{eg}{\Lambda^2} \left(g^{\mu\lambda} - \frac{q^\mu q^\lambda}{q^2} \right) \bar{u}^{s'}(p') \gamma_\lambda \gamma^5 u^s(p) \bar{v}^{r'}(k') \left[F_1(q^2) \gamma_\mu + \frac{i}{2m_e} F_2(q^2) \sigma_{\mu\nu} q^\nu \right] v^r(k). \tag{3.46}$$

In the non-relativistic limit, we can expand the spinors in accordance with Nobile et. al. [18]. This allows us to arrive at the final expression for the scattering amplitude for the anapole interaction

$$\mathcal{M} = \frac{4eg}{\Lambda^2} m_\chi m_e \left[2 \left(\mathbf{v}^\perp_{\mathrm{el}} \cdot \xi^{s'\dagger} \mathbf{S}_\chi \xi^s \right) \delta^{r'r} + g_e \left(\xi^{s'\dagger} \mathbf{S}_\chi \xi^s \right) \cdot \left(i \frac{\mathbf{q}}{m_e} \times \eta^{r'\dagger} \mathbf{S}_e \eta^r \right) \right] \tag{3.47}$$

where we have identified the electron g-factor g_e as well as the spin operators $\mathbf{S}_\chi = \boldsymbol{\sigma}/2$ where $\boldsymbol{\sigma}$ is the vector consisting of the three Pauli spin matrices. Furthermore, ξ and η are the two-component spinors for the dark matter particle and the electron respectively. As we can see in (3.47), a theory where the scattering amplitude

depends only on the momentum transfer is not enough. The scattering amplitude for the anapole interaction depends also on $\mathbf{v}_{\mathrm{el}}^{\perp}$. One may also compare the expression (3.47) to the operators listed in Table 3.1 to find that the anapole amplitude is actually a superposition of the operators $\mathcal{O}_8$ as the first term, and $\mathcal{O}_9$ as the second. The anapole interaction is thus a perfect example for why a more general description is necessary. Writing the general scattering amplitude as (3.26) is therefore a better approach compared to writing just $\mathcal{M}(\mathbf{q})$.

3.5 Scattering with atoms

So far, we have introduced a general framework for studying the interactions between dark matter particles and electrons. We found the rate at which dark matter particles alter the states of electrons (3.24). We also showed the necessity of using a more general interaction framework by calculating the scattering amplitude for anapole interactions (3.47). This general framework is described by the squared transition amplitude (3.30). The task remaining is now to find the rate at which dark matter particles actually ionise atoms. This is what will be observable in a detector.

We start off by making a slight change of notation. Since we will now be discussing electrons bound to atoms, it is useful to consider a notation that incorporates the specific quantum numbers of the given state. So we write $\psi_1 = \psi_{nlm}$ for the initial electron state, and $\psi_2 = \psi_{k'l'm'}$ for the final electron state. Here, (n, l, m) denotes the principal, angular and magnetic quantum numbers for the bound electron, and (k', l', m') denotes the asymptotic momentum, angular and magnetic quantum numbers for the free electron. We also want to find the relation between the ionisation rate R_{ion}^{nl} for the (n, l) orbital and the total transition rate $R_{1\to 2}$ from (3.24). In an article by Essig et. al. [19] the authors define an integral operator

$$\frac{1}{2}\sum_{l'=0}^{\infty}\sum_{m'=-l'}^{l'}\int\frac{k'^3\mathrm{d}\ln E_e}{(2\pi)^3} \tag{3.48}$$

where $E_e = k'^2/2m_e$ is the energy of the ionised electron. Acting on the total transition rate $R_{1\to 2}$ with the integral operator (3.48) accounts for the contribution to R_{ion}^{nl} from all allowed final electron states with momenta in the range $\mathbf{k}'$ and $\mathbf{k}' + \mathrm{d}\mathbf{k}'$. Summing over all initial states gives the total ionisation rate for the (n, l) orbital as

$$R_{\mathrm{ion}}^{nl} = \sum_{m=-l}^{l}\sum_{l'=0}^{\infty}\sum_{m'=-l'}^{l'}\int V\frac{k'^3\mathrm{d}\ln E_e}{(2\pi)^3}R_{1\to 2}. \tag{3.49}$$

Note that we have multiplied by a factor of 2 to account for spin degeneracy, as well as a factor of V which compensates for the normalisation of the electron wave functions. We may now get the ionisation spectrum, or the differential ionisation rate, as

$$\frac{\mathrm{d}R_{\mathrm{ion}}^{nl}}{\mathrm{d}\ln E_e} = \sum_{m=-l}^{l} \sum_{l'=0}^{\infty} \sum_{m'=-l'}^{l'} \frac{Vk'^3}{(2\pi)^3} R_{1\to 2}. \tag{3.50}$$

Looking at the total transition rate (3.24) we see a dependence on the transition amplitude (3.30). Since we are now specialising to the case of ionised electrons, it becomes relevant to define a squared ionisation amplitude instead. We define this as

$$\left|\mathcal{M}_{\mathrm{ion}}^{nl}\right|^2 = \frac{4Vk'^3}{(2\pi)^3} \sum_{m=-l}^{l} \sum_{l'=0}^{\infty} \sum_{m'=-l'}^{l'} \left|\mathcal{M}_{1\to 2}\right|^2. \tag{3.51}$$

It is also possible to write $\left|\mathcal{M}_{\mathrm{ion}}^{nl}\right|^2$ in terms of $\mathcal{M}$. The prefactor as well as the sums are then included in the expression (3.30). If we define the dimensionless ionisation form factor

$$\left|f_{\mathrm{ion}}^{nl}(k',q)\right|^2 = \frac{4Vk'^3}{(2\pi)^3} \sum_{m=-l}^{l} \sum_{l'=0}^{\infty} \sum_{m'=-l'}^{l'} \left|f_{1\to 2}(q)\right|^2 \tag{3.52}$$

we can write (3.51) in terms of $\left|\mathcal{M}(\mathbf{v}_{\mathrm{el}}^{\perp}, \mathbf{q})\right|^2$ such that

$$\begin{aligned} \left|\mathcal{M}_{\mathrm{ion}}^{nl}\right|^2 = \Bigg\{ & \left|\mathcal{M}(\mathbf{v}_{\mathrm{el}}^{\perp}, \mathbf{q})\right|^2 \left|f_{\mathrm{ion}}^{nl}(k',q)\right|^2 \\ & + \frac{4Vk'^3}{(2\pi)^3} \sum_{m=-l}^{l} \sum_{l'=0}^{\infty} \sum_{m'=-l'}^{l'} \Bigg(m_e^2 \left|\nabla_{\mathbf{k}} \mathcal{M}(\mathbf{v}_{\mathrm{el}}^{\perp}, \mathbf{q}) \cdot \mathbf{f}_{1\to 2}(\mathbf{q})\right|^2 \\ & + 2m_e \mathcal{R}\left[\mathcal{M}(\mathbf{v}_{\mathrm{el}}^{\perp}, \mathbf{q}) f_{1\to 2}(\mathbf{q}) \nabla_{\mathbf{k}} \mathcal{M}(\mathbf{v}_{\mathrm{el}}^{\perp}, \mathbf{q}) \cdot \mathbf{f}_{1\to 2}^{*}(\mathbf{q})\right] \Bigg) \Bigg\}_{\mathbf{k}=0}. \end{aligned} \tag{3.53}$$

This way of writing the ionisation amplitude reveals another property of the general framework for dark matter-electron interactions. In fact, we are able to write (3.53) in a more general form

$$\left|\mathcal{M}_{\mathrm{ion}}^{nl}\right|^2 = \sum_{i=1}^{4} R_i^{nl}\left(\mathbf{v}_{\mathrm{el}}^{\perp}, \frac{\mathbf{q}}{m_e}\right) W_i^{nl}(k', \mathbf{q}). \tag{3.54}$$

Here, $R_i^{nl}\left(\mathbf{v}_{\mathrm{el}}^{\perp}, \frac{\mathbf{q}}{m_e}\right)$ are the dark matter response functions, which are determined by the nature of the interaction and contain the coupling constants for the interactions listed in Table 3.1, and $W_i^{nl}(k', \mathbf{q})$ are the atomic response functions which are determined by the initial and final electron wave functions. These response functions are one of the main results of the article written by Catena et. al. [3]. Furthermore, the atomic response function $W_1^{nl}(k', \mathbf{q})$ is equal to the ionisation form factor (3.52) which has been studied in previous works, while the responses for $i = 2, 3, 4$ are the ones generated by the framework of general dark matter-electron interactions and were not considered until this point. The details of these response functions are summarised in the article by Catena et. al., however, it is important to note that the atomic response functions for $i = 2, 3, 4$ depend on the vectorial form factor

(3.33) as well as $\mathbf{q}/m_e$, and that writing the squared ionisation amplitude in terms of the response functions is useful for numerical calculations.

So if we now rewrite the total transition rate (3.24) to include the ionisation amplitude (3.51) we get

$$\frac{\mathrm{d}R^{nl}_{\mathrm{ion}}}{\mathrm{d}\ln E_e} = (2\pi)\delta(E_f - E_i)\frac{n_\chi}{16 m_\chi^2 m_e^2}\int \frac{\mathrm{d}^3 q}{(2\pi)^3}\int \mathrm{d}^3 v\ f_\chi(\mathbf{v})\frac{1}{4}\left|\mathcal{M}^{nl}_{\mathrm{ion}}\right|^2 \tag{3.55}$$

where the factor of $1/4$ compensates for the factor 4 in the definition of the ionisation amplitude (3.51). The energy difference between the initial and final state is actually given by (3.5). If we expand the integral over the momentum transfer as

$$\int \frac{\mathrm{d}^3 q}{(2\pi)^3} = \int \mathrm{d}\Omega \int \frac{\mathrm{d}q}{(2\pi)^3} q^2 = \int \mathrm{d}\phi \int \mathrm{d}\cos\theta_{qv} \int \frac{\mathrm{d}q}{(2\pi)^3}, \tag{3.56}$$

we can integrate (3.55) over ϕ as well as $\cos\theta_{qv}$ to find that

$$\frac{\mathrm{d}R^{nl}_{\mathrm{ion}}}{\mathrm{d}\ln E_e} = \frac{n_\chi}{128\pi m_\chi^2 m_e^2}\int \mathrm{d}q\ q \int \frac{\mathrm{d}^3 v}{v} f_\chi(\mathbf{v})\Theta(v - v_{\mathrm{min}})\left|\mathcal{M}^{nl}_{\mathrm{ion}}\right|^2 \tag{3.57}$$

where we implement the Heaviside step function $\Theta(v - v_{\mathrm{min}})$, identifying the minimum velocity $v_{\mathrm{min}} = v\cos\theta_{qv} = \Delta E_{1\to 2}/q + q/2m_e$. The ionisation spectrum (3.57) gives the ionisation rate as a function of the transferred electron energy E_e. The rate also depends on properties of the atom, embedded in $\left|\mathcal{M}^{nl}_{\mathrm{ion}}\right|^2$, which also contains the initial and final electron wave functions. So given the initial dark matter particle parameters, as well as specifying the electron wave functions, one may perform the integrals and find the ionisation rate as a function of the transferred electron energy. This is the signal produced by the theory. Since a detector measures the total event rate, it is necessary to perform statistical studies in order to distinguish between a background event and a signal produced by this model.

4

Statistics

In this chapter we will follow calculations performed in an article by Cowen et. al. [20] that will be relevant for our statistical analysis. The statistical framework will be laid out in such a way that every tool needed to perform hypothesis testing of new physics, and express the results in terms of statistical significance will be presented. The chapter begins with a section presenting the statistical foundations of our study. Later in this chapter, the framework is applied in a way that enables us to distinguish between a null, background only, hypothesis and an alternative, background plus signal, hypothesis. The different hypotheses will therefore be representing the case where our model produces no signal, or background signals only, as well as our model producing a signal in addition to the background events. Worth noting is that a similar calculation is performed in an article by Catena et. al. [21] where the authors instead focus on semiconductor crystals as targets.

4.1 Statistical methods for hypothesis testing

The statistical analysis will be based on a sampled data set $\mathbf{D}$. In order to perform hypothesis testing based on this data set we need to define a null hypothesis as well as an alternative hypothesis. We do this as follows:

- The **null hypothesis** is defined by setting to zero all coupling constants for the interaction operators in Table 3.1. This corresponds to having only background events in a hypothetical dark matter experiment searching for atomic ionisations.
- The **alternative hypothesis** is defined by setting to a value different from zero a coupling in Table 3.1. This means that, on top of the background events, there will be a signal in alignment with (3.57).

The two different hypotheses will form a corresponding test statistic, which we will denote by q. The distribution of the test statistics will in turn be used to determine the statistical significance with which the null hypothesis can be rejected in favour of the alternative one. Notice that q and its probability density function depend on the data set for the underlying hypothesis. As a first step, we will describe the data set $\mathbf{D}$ for each hypothesis. We do this by considering a set of n bins, such that $\mathbf{D} = (N_1, ..., N_n)$. Each entry N_i in the data set has an associated expectation value μ_i, such that in the ith bin, the expectation value is

$$\mu_i = s_i + b_i. \tag{4.1}$$

Here, s_i denotes the signal produced by the model under the hypothesis in question,

and b_i denotes the background.

Given the expectation value μ_i one may now sample the data set $\mathbf{D}$. The relation between N_i and μ_i is given such that the data set entry is an integer randomly sampled from a Poisson distribution with the mean value μ_i

$$f(k;\mu_i) = \frac{\mu_i^k e^{-\mu_i}}{k!}. \tag{4.2}$$

This means that $N_i \in f(k;\mu_i)$. These Poisson numbers are used to form the so called likelihood L. The likelihood is defined as a product of Poisson distributions

$$L(\mathbf{D}|\theta) = \prod_{i=1}^{n} \frac{\mu_i^{N_i}}{N_i!} e^{-\mu_i}. \tag{4.3}$$

Here, we write θ as the parameter that determines the signal s_i such that $s_i = s_i(\theta)$. The likelihood is used to find the profile likelihood ratio defined as

$$\lambda = \frac{L(\mathbf{D}|0)}{L(\mathbf{D}|\hat{\theta})}. \tag{4.4}$$

Here, the numerator corresponds to the likelihood found by setting the signal to zero. Thus, in this case, the likelihood only depends on the background. The denominator, on the other hand, corresponds to the maximum likelihood as a function of the parameter θ. So in order to find the denominator one must search for the parameter $\hat{\theta}$ that maximises (4.3). The profile likelihood ratio now gives a point in the test statistic distribution as

$$q = -2\ln\lambda. \tag{4.5}$$

The fact that this is only one point in the distribution of q arises from the random sampling of the data set $\mathbf{D}$. For every sampled data set, there will be a point in the test statistic distribution corresponding to that data set. Since the entries of $\mathbf{D}$ are randomly sampled from a Poisson distribution, one may expect various values for (4.5) and thus forming some distribution. The test statistic distribution is however different depending on which hypothesis the data is sampled under. When sampling data under the null hypothesis, one expects a so called half chi-square distribution, or $\frac{1}{2}\chi^2$ [20]. For this distribution f_{null}, half of the values line up at precisely zero, while the other half follow a chi-square distribution

$$f_{\text{null}}(q_{\text{null}}) = \frac{1}{2}\delta(q_{\text{null}}) + \frac{1}{2}\frac{1}{\sqrt{2\pi}}\frac{1}{\sqrt{q_{\text{null}}}}e^{-q_{\text{null}}/2}. \tag{4.6}$$

Here, q_{null} is one of the values of q sampled from data generated under the null hypothesis $\mathbf{D}_{\text{null}}$. This data set is sampled according to (4.2) with $\mu_i = b_i$. So one assumes that the expected amount of signals per bin is entirely dependent on the background. On the contrary, the data set $\mathbf{D}_{\text{alt}}$ is sampled under the alternative hypothesis which follows (4.2) precisely with $s_i^{\bar{\theta}} \neq 0$ where $\bar{\theta}$ is the value of θ that characterises the alternative hypothesis. The data set for the alternative hypothesis forms the test statistic q_{alt}. The distribution of q_{alt} is used to determine the p-value for discovery. This is done according to

$$p = \int_{q_{\text{med}}}^{\infty} \mathrm{d}q_{\text{null}}\ f_{\text{null}}(q_{\text{null}}) \tag{4.7}$$

where q_{med} is the median value of the probability density function of q_{alt}, i.e. f_{alt}. So integrating the distribution of the null hypothesis test statistic from the median value of f_{alt} up to infinity gives the p-value. In turn, the p-value is related to the statistical significance $\mathcal{Z}$ through

$$\mathcal{Z} = \Phi^{-1}(1-p) \tag{4.8}$$

where Φ is the cumulative distribution function of a Gaussian probability density with mean 0 and variance 1. Notice that this is a function of $\bar{\theta}$. If a specific statistical significance $\mathcal{Z}^*$ is desired, one solves for $\bar{\theta}$ in the equation $\mathcal{Z}(\bar{\theta}) = \mathcal{Z}^*$.

4.2 Hypothesis testing of new physics

The statistical theory presented will be applied to study the physics model presented within this thesis. We do this by considering the signal to arise from (3.57). Since this is a function of energy, we define the signal as

$$s_i = \mathcal{E} \int_{E^i_{e,1}}^{E^i_{e,2}} \mathrm{d}E_e \frac{\mathrm{d}R^{nl}_{\text{ion}}}{\mathrm{d}E_e} \tag{4.9}$$

where the region $[E^i_{e,1}, E^i_{e,2}]$ represents the ith energy bin, and $\mathcal{E}$ is the so called effective exposure for the detector. The exposure for a detector is defined as the volume of the detector material multiplied by the target density as well as the time during which the experiment is running. The difference between exposure and effective exposure is that the latter contains a factor which is determined by the efficiency of the detector. Integrating over the electron energy as well as multiplying by the exposure thus produces the rate in the ith bin. We then form the expectation value according to (4.1) and perform the sampling for the data from the Poisson distribution (4.2). When implementing our model, there will be two parameters that determine the signal, the dark matter particle mass m_χ and the coupling constant for a given interaction operator c_j. By fixing the mass, we are free to perform the statistical analysis using the coupling constant as the free parameter and we can form the likelihood for a specific data set as a function of the coupling constant

$$L(\mathbf{D}|c_j) = \prod_{i=1}^{n} \frac{\mu_i^{N_i}}{N_i!} e^{-\mu_i} \tag{4.10}$$

where $\mu_i = s_i(c_j) + b_i$. This means that the likelihood profile ratio takes the form

$$\lambda = \frac{L(\mathbf{D}|0)}{L(\mathbf{D}|\hat{c}_j)}. \tag{4.11}$$

In the profile likelihood ratio, the parameter that is used to maximise the likelihood in the denominator is now the coupling constant c_j. The data set $\mathbf{D}_{\text{alt}}$ will be sampled from a benchmark point in parameter space characterised by $c_j = \bar{c}_j$, assuming that one operator at a time contributes to the ionisation rate. The data set for the

null hypothesis, however, will be sampled from $c_j = 0$. This effectively removes all interactions and sets the signal to zero. From all this it is possible to form the two test statistic distributions for q_{null} and q_{alt}. The test statistic q_{null} will follow the $\frac{1}{2}\chi^2$ distribution (4.6), while q_{alt} will obey a distribution depending on both the mass as well as the interaction operator. The process for extracting the p-value is analogous to what has been described above. For a given $\bar{c}_j$, we tabulate all values q_{alt} in order of magnitude, and then find the median which serves as one of the limits for which (4.6) is integrated. The p-value is then used to find the statistical significance of $\bar{c}_j$ according to (4.8).

As stated, this analysis is performed for a given dark matter particle mass m_χ and $\bar{c}_j$. We then iterate over $\bar{c}_j$ and solve $\mathcal{Z}(\bar{c}_j) = \mathcal{Z}^*$ numerically. The outcome of the statistical analysis performed in this chapter is the smallest coupling constant c_j at which a dark matter particle of mass m_χ is detectable with a statistical significance of $\mathcal{Z}$.

5

Numerical Implementation

Producing limits for the sensitivity of a detector requires numerical simulations. This chapter presents how we implement the model described in the previous chapters. We also describe how we perform the hypothesis testing using the statistical framework described. The numerical implementation utilises an existing code package [3]. All implementation is done using C++.

5.1 Computing tools

For simulating the data presented in the article by Catena et. al. [3], the authors used a code package written in C++. This package allows the user to simulate the ionisation rates of xenon and argon targets induced by dark matter particles. By defining parameters such as the integration limits, dark matter particle mass, as well as interaction operator and the corresponding coupling constant, one may integrate the expression (3.57). In doing this, we find the total number of events. If we do this for a given mass, we are able to produce a spectrum as the ones shown in Figure 5.1.

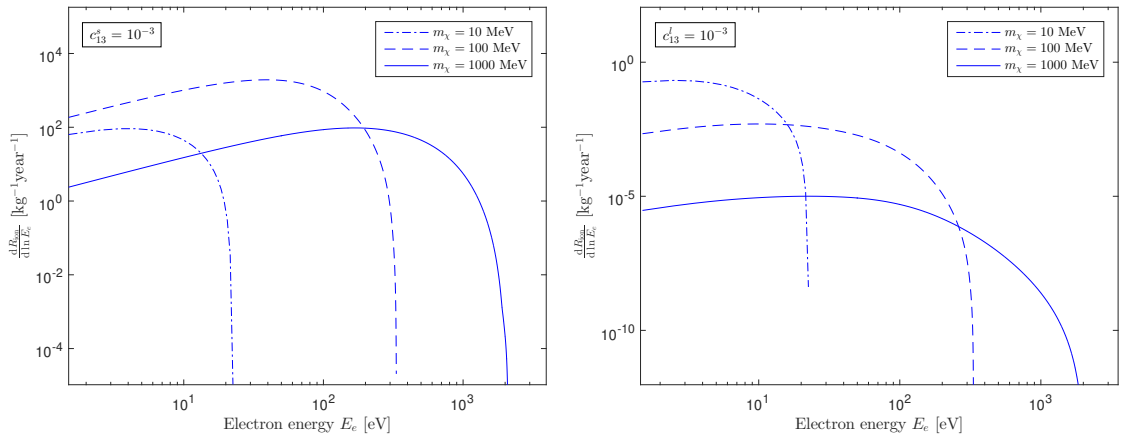

(a) Short-range interaction. **(b)** Long-range interaction.

Figure 5.1: Figures showing the spectra (3.57) for dark matter particles of masses $10, 100$ and 1000 MeV interacting with xenon bound electrons through $\mathcal{O}_{13}$ with a coupling constant $c_{13} = 10^{-3}$. Figure 5.1a shows the spectra under the assumption of short-range interactions, and Figure 5.1b shows the spectra for long-range interactions.

Here, we show the spectra for dark matter particle masses of $10, 100$ and 1000 MeV. We assume that dark matter interacts with electrons through the interaction operator $\mathcal{O}_{13}$. Figure 5.1a shows the spectra for the three masses under short-range interactions with a coupling constant $c_{13}^s = 10^{-3}$ and Figure 5.1b shows the spectra under long-range interactions with a coupling constant $c_{13}^l = 10^{-3}$. Both sets of spectra assume a xenon target. By dividing the energy spectrum into a set of energy bins, we can extract the number of events per energy bin. The number of events in the ith bin corresponds to the signal expectation value s_i as mentioned in (4.1).

5.2 Statistical simulations

Finding the statistical significance for a data set can be done by following the recipe given in Chapter 4. This does however include the process of maximising the likelihood in the denominator of (4.11) as well as evaluation of the statistical significance itself. Furthermore, one may seek a specific value for $\mathcal{Z}$. As a result, one may need to perform many simulations in order to extract results. The code used to find the statistical significance for a data set has been written with this in mind.

A function has been written for finding the statistical significance of a data set. This function is called `Significance()` and takes the mass m_χ, an arbitrary value for the coupling constant $c_j = \bar{c}_j$ as well as the target atom type as input. With these input variables, one may specify the interaction operator $\mathcal{O}_j$. One must also specify integration limits as well as the bin size for the electron recoil energy. With all this, a so called fiducial spectrum is produced. This is done by integrating the spectrum using a fiducial coupling constant $c_j = c_f = 1$. The reason for this is to avoid integration multiple times. Since we study the effects of one interaction operator at a time, the coupling constant simply acts as a rescaling parameter for the total spectrum. In other words, in order to find the spectrum for a coupling constant one simply has to multiply the fiducial spectrum by the coupling constant squared. So the signal within each bin has to be evaluated only once.

The next step is to produce the data sets $\mathbf{D}_{\text{null}}$ and $\mathbf{D}_{\text{alt}}$. To do this, we sample data according to (4.2). This is done using the function `Poisson_Sample()` which takes a vector with the expectation value for each bin as input. When sampling data for the null hypothesis, the input vector is simply the vector of background signals b_i. The background signal can be set to values measured in experiments. When sampling data for the alternative hypothesis we use instead the vector of expectation values μ_i. This expectation value is found by multiplying the fiducial spectrum by c_j^2 and then adding the background signal b_i. The expectation value produced in doing this is assumed to be the real signal, the one seen in nature.

With the data produced, we now want to find the likelihood, and in turn the test statistic q. There is a way of rewriting the expression for the test statistic (4.5), by applying the logarithm to the likelihood ratio. One finds that

$$q = -2\left[\sum_{i=1}^{n}\left(N_i \ln b_i - b_i\right) - \sum_{i=1}^{n}\left(N_i \ln\left(s_i + b_i\right) - \left(s_i + b_i\right)\right)\right], \tag{5.1}$$

which produces q_{null} when using the data set for the null hypothesis and q_{alt} when using the data set for the alternative hypothesis. The first term in the expression corresponds to the logarithm of the numerator of the profile likelihood ratio (4.11) while the second term corresponds to the logarithm of the likelihood in the denominator. The negative sign arises from division of two logarithms. Since the second term corresponds to $L(\mathbf{D}|\hat{c}_j)$ it has to be maximised.

The maximisation process is done using a method which can be found in Numerical Recipes [22]. This method is called the Golden Section Search. It finds the value of a parameter that minimises a function. Since minimising a function is the same as maximising the same function but negative, we choose to minimise the function $-\ln L(\mathbf{D}|\hat{c}_j)$. We define this as the function called `NegativeLoglikelihood()`. This function takes the fiducial spectrum as input, as well as the data set $\mathbf{D}$ for the hypothesis being simulated. This function depends on the coupling constant. Since the function for $-\ln L(\mathbf{D}|\hat{c}_j)$ imports the fiducial spectrum, we are not required to perform the integral every time the coupling constant is updated. The function `Loglikelihood()` simply rescales the spectrum, evaluates the second term of (5.1) and returns the value.

The Golden Section Search method has two parts. The first part finds an interval which contains the minimum of a function. This function is called `golden.bracket()` and takes two initial brackets as input, as well as the function to be minimised. When this is done, one simply calls the function `golden.minimize()` which takes as input the function to be minimised and returns the parameter that minimises the function.

The Golden Section Search enables us to find the coupling constant that maximises the likelihood $\ln L(\mathbf{D}|\hat{c}_j)$ for a given data set $\mathbf{D}$. Thus we are able to extract the test statistic q. In order to form distributions for q_{null} and q_{alt} we repeat the process by sampling data multiple times and evaluating the expression (5.1) for each data set.

Having found the distributions for the test statistics we want to find the median of the distribution for q_{alt}. We do this by calling the `sort()` function in the `algorithm` library. This function rearranges the elements of a vector in order from the smallest value in the vector to the largest. By doing this, one can simply find the median q_{med} as the value stored in the middle place of the vector storing the values for q_{alt}. If the vector has an even amount of entries, q_{med} will instead be the average of the two middle values.

In order to find the statistical significance for a data set we would have to find the p-value. Cohen et. al. [20] show that one can relate the statistical significance to the median q_{med} such that

$$\mathcal{Z} = \Phi^{-1}(1-p) = \sqrt{q_{\text{med}}}. \tag{5.2}$$

This means that fewer computations are needed to find the statistical significance for a data set. This is the value that the function `Significance()` returns.

Typically, one is interested in finding a point in parameter space that corresponds to a specific statistical significance. In the scope of this thesis, we are interested in the lowest detectable coupling constant corresponding to a specific dark matter particle mass under a given interaction operator $\mathcal{O}_j$. In order to find the coupling constant that corresponds to a statistical significance for $\mathcal{Z} = 3$ we solve the equation $\mathcal{Z} - 3 = 0$. This is done using a function from the pre-existing code package called `Find_Root()` which takes as input the function for which we find the root, along with two values that bracket the parameter which gives the root as well as a precision parameter. The function returns the parameter that solves the equation. By using this function to solve the equation $\mathcal{Z} - 3 = 0$ we are able to find the coupling constant that corresponds to a specific mass with a statistical significance of $\mathcal{Z} = 3$.

5.3 Parameters for a theoretical experiment

Recently, data from the XENON1T experiment has been revisited, where the authors study the constraints of the experiment and others like it [11]. Since the experiment has concluded however, the experiment XENONnT will be the next upgrade for XENON1T. In order to perform a theoretical experiment for XENONnT we will assume the same background signal as for XENON1T. An appropriate background to assume is a flat background rate of 1 event/(day $\times$ tonne $\times$ keV) which is the experimental background for XENON1T in the electron recoil energy region of $E_e \in [0.2, 3.0]$ keV. This means that the number of background events in each bin will be the same, where the bin size will determine the value for b_i. As for the exposure, we assume an effective exposure four times larger than that of XENON1T, or 4×22 tonne-days, which is the projected exposure for XENONnT. The dark matter particle is assumed to be a Majorana fermion with spin $\frac{1}{2}$. The type of interaction will focus on a few examples that are generated by a general dark matter-electron interaction framework. Thus interaction operators $\mathcal{O}_1$ and $\mathcal{O}_4$ will be omitted, while a few interactions depending only on the momentum transfer will be included for illustratory reasons.

6
Results

This chapter presents the results of simulations performed in accordance with the previous chapter. We present the smallest detectable coupling constants for a corresponding dark matter particle mass under different interaction operators. The detector properties used for producing the results resemble those of the future XENONnT experiment. We also study the effects of lowering the detectable electron recoil energy.

6.1 Test statistic distributions

When performing the simulations, the electron recoil energy range was divided into 20 bins of equal size. For an energy range of 0.2 keV − 3.0 keV the energy bin width is 140 eV. For the purpose of illustration, using 1000 points for the distributions of q_{null} and q_{alt} respectively, at the mass m_χ that corresponds to the smallest detectable coupling constant for short-range and long-range interactions under $\mathcal{O}_{13}$, the distributions for the test statistics are shown in Figure 6.1.

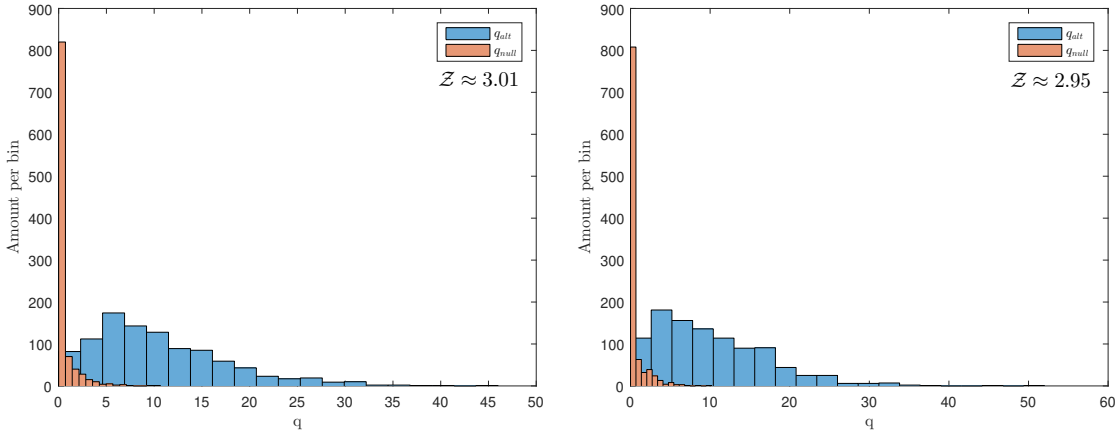

(a) Short-range interaction. **(b)** Long-range interaction.

Figure 6.1: Figure showing the distributions for the test statistics q_{null} and q_{alt}. The distributions in Figure 6.1a are produced under short-range interactions for $\mathcal{O}_{13}$ and the mass $m_\chi = 300$ MeV. The distributions in Figure 6.1b are produced under long-range interactions for the same interaction operator, but with the mass $m_\chi = 200$ MeV. The distributions are the result of the process of finding the coupling constant corresponding to a statistical significance $\mathcal{Z} \approx 3$ for the given mass m_χ.

6.2 Sensitivity of XENONnT

For simulating the experiments with XENONnT we instead use 100 points for the test statistics in order to speed up simulations. The bin width remains at 140 eV, and the experiment is simulated under a few different interaction operators found in Table 3.1. For each operator, the experiment is simulated under both the assumption that the interaction is short-ranged and long-ranged. By finding the coupling constants for 50 different masses that corresponds to $\mathcal{Z} \approx 3$ with the detector parameters of XENONnT we can produce Figure 6.2.

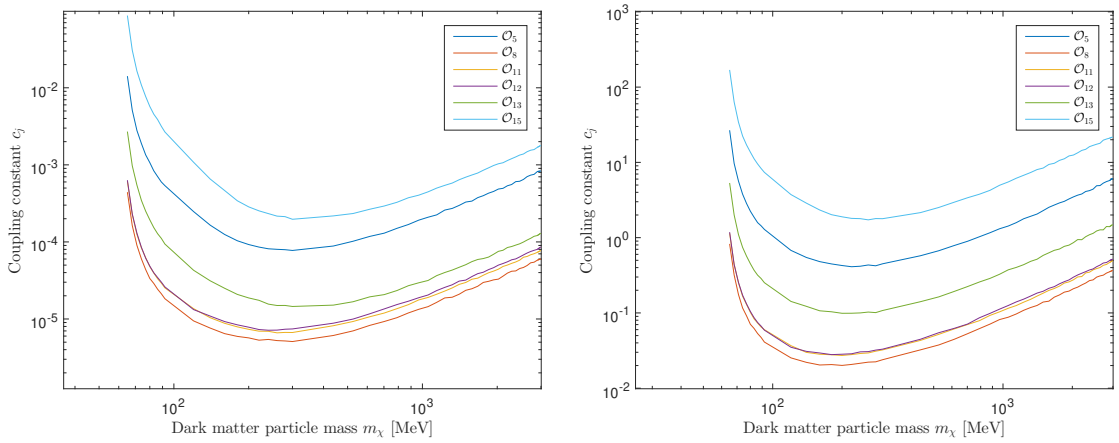

(a) Short-range interactions.

(b) Long-range interactions.

Figure 6.2: Figure showing the smallest coupling constant that can be detected as a function of the dark matter particle mass with a statistical significance $\mathcal{Z} \approx 3$ in the XENONnT experiment. Figure 6.2a shows the projected sensitivity for XENONnT under the assumption of short-range interactions for operators $\mathcal{O}_5, \mathcal{O}_8, \mathcal{O}_{11}, \mathcal{O}_{12}, \mathcal{O}_{13}$ and $\mathcal{O}_{15}$. Figure 6.2b shows the projected sensitivity for XENONnT under the assumption of long-range interactions for the same interaction operators.

Each point in the parameter space of Figure 6.2 is simulated in such a way that each individual point has a test statistic distribution like the ones shown in Figure 6.1. Note that interaction operators $\mathcal{O}_1$ and $\mathcal{O}_4$ are left out since they do not depend on either $\mathbf{q}$ or $\mathbf{v}_{\text{el}}^{\perp}$.

6.3 Improvements for future experiments

If one instead considers a theoretical experiment where the range for the electron recoil energy is increased at the lower boundary it is possible to probe smaller masses. To show this, we keep the upper boundary for E_e and extend the lower boundary from 0.2 keV to 0.02 keV. By keeping the amount of energy bins the same, this means that each energy bin now has a width of 149 eV. Assuming that the background signal remains flat at a rate of 1 event/(day $\times$ tonne $\times$ keV) and by keeping the exposure the same as for XENONnT we find the projected sensitivity for such an experiment in Figure 6.3.

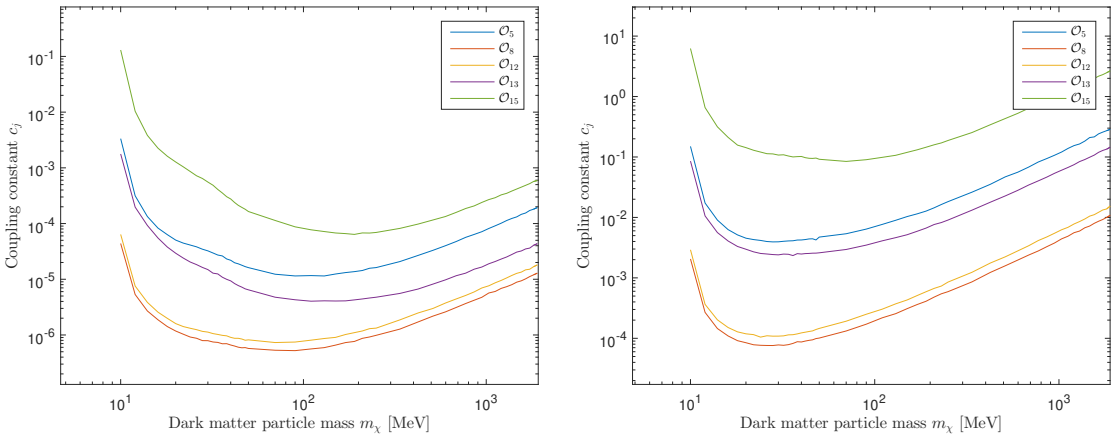

(a) Short-range interactions.

(b) Long-range interactions.

Figure 6.3: Figure showing the smallest coupling constant that can be detected as a function of the dark matter particle mass with a statistical significance $\mathcal{Z} \approx 3$ in an experiment similar to XENONnT, but with an increased energy range. Figure 6.3a shows the projected sensitivity for such an experiment under the assumption of short-range interactions for the operators $\mathcal{O}_5, \mathcal{O}_8, \mathcal{O}_{12}, \mathcal{O}_{13}$ and $\mathcal{O}_{15}$. Figure 6.3b shows the projected sensitivity for the theoretical experiment under the assumption of long-range interactions for the same operators.

Just as for Figure 6.2, each point in the parameter space has an associated test statistic distribution similar to the ones shown in Figure 6.1.

7

Discussion and Conclusion

In this chapter, we analyse the results from the simulations as well as comment on specific choices of certain parameters. We will also discuss and motivate the approximations made as well as the limitations for this thesis.

7.1 The numerical calculations

To assure ourselves that the numerical calculations are performed correctly we present examples of the test statistic distributions in Figure 6.1. The distributions shown correspond to the test statistics that produce a statistical significance $\mathcal{Z} \approx 3$ for two different dark matter particle masses. It is important that the distributions for q_{null} and q_{alt} follow $\frac{1}{2}\chi^2$ and χ^2 distributions respectively, in agreement with Cohen et. al. [20]. One important feature to note is that the statistical significance is not exactly equal to three. This is due to the fact that the function `Find_Root()` searches for a value $\mathcal{Z}$ that solves the equation $\mathcal{Z} - 3 = 0$ as a function of the coupling constant up to a certain error. Numerically, it will never be possible to solve the equation $\mathcal{Z} - 3 = 0$ exactly, so one is forced to set an acceptable threshold at which the significance is deemed to be close enough to the desired value.

In Figure 6.1 we have used 1000 points for each distribution for illustrative purposes. When performing simulations for the sensitivity for XENONnT we instead change this to 100. Using more points in the test statistic distributions adds more precision to the numerical calculations, however, the run time is also increased. The run time for the calculations scale linearly with the amount of points in the test statistic distributions. So when simulating the sensitivity for XENONnT, 100 points was deemed to provide good enough precision without compromising the run time too much. The run time also increases with the amount of masses used. For all simulations for the sensitivity, we use 50 dark matter particle masses, which we distribute in a way such that there are more points in the lower mass region compared to the high mass region. We do this since, in the low mass region, the smallest detectable coupling constant is very prone to fluctuations for small changes in the dark matter particle mass. Including more points in the high mass region would only serve to reduce the fluctuations in the sensitivity slightly. Another thing that affects the run time is the number of energy bins that (4.9) is integrated over. The choice of having 20 energy bins was deemed to provide good enough precision while still keeping the run time at an acceptable level. With all settings mentioned, the simulations have to be performed for one interaction operator at a time. One such simulation could

take approximately three hours.

The parameter choices mentioned above make the sensitivity prone to some numerical error. Clearly, by looking at Figure 6.2 as well as Figure 6.3 there is a small amount of noise. However, this is not only caused by the way we restrict our numerical precision. One has to keep in mind that we also randomly sample data numerically from a Poisson distribution (4.2). Due to the random nature of this sampling, no two data sets will be alike. This also means that we include some statistical error, which adds to the noise in the sensitivity.

It is worth noting that the dark matter particle mass could also be a free parameter. This would however require a two-dimensional minimisation in order to produce the sensitivity for XENONnT. Instead, we choose to simply scan the sub-GeV region for the dark matter particle mass.

7.2 The projected sensitivity for XENONnT

For producing the projected sensitivity for XENONnT we choose a selection of interaction operators. Specifically, we are interested in interactions that are generated by the general dark matter-electron interaction framework. Thus, interaction operators containing $\mathbf{v}_{\text{el}}^{\perp}$ in particular are of interest. When studying the results in Figure 6.2 the first thing one may notice is the splitting for the sensitivity for different interaction operators. The simulations tell us that the interaction operator $\mathcal{O}_8$ has the best chances of being observed in XENONnT, with operators $\mathcal{O}_{11}$ and $\mathcal{O}_{12}$ following. Referring to Table 3.1 we can see that the chances of being detected in XENONnT is directly correlated to the powers of $\mathbf{q}$ and $\mathbf{v}_{\text{el}}^{\perp}$ that the interaction operator exhibits. Operator $\mathcal{O}_8$ only has two explicit dependencies, namely $\mathbf{S}_\chi$ and $\mathbf{v}_{\text{el}}^{\perp}$. The interaction that has second to best chances of being detected, on the other hand, depends on $\mathbf{q}/m_\chi$ and not on the perpendicular velocity vector. Since the interaction operators $\mathcal{O}_8$ and $\mathcal{O}_{11}$ only differ on this one point, we can conclude that interactions depending on the momentum transfer vector have a lower chance of being visible in the XENONnT experiment compared to interactions that depend on $\mathbf{v}_{\text{el}}^{\perp}$ in the same way. Comparing the detection limits for operators $\mathcal{O}_{11}$ and $\mathcal{O}_{12}$ show that they are very similar, and hardly distinguishable. Instead of the transfer momentum, interaction operator $\mathcal{O}_{12}$ depends on $\mathbf{S}_e \times \mathbf{v}_{\text{el}}^{\perp}$. Due to the sensitivity to both these interactions being so similar, one can draw the conclusion that $\mathbf{q}/m_\chi$ and $\mathbf{S}_e \times \mathbf{v}_{\text{el}}^{\perp}$ affect detectability almost equally. Looking at the sensitivity for detecting an interaction under operator $\mathcal{O}_{15}$ we see that this would be the most difficult type of interaction to detect. Based on the previous statements, this is not surprising. The operator $\mathcal{O}_{15}$ includes all possible degrees of freedom that we allow our model. The interaction depends on the spin of both particles in the scattering process, as well as being linear in $\mathbf{v}_{\text{el}}^{\perp}$ and second order in $\mathbf{q}$. When introducing the interaction operators in Table 3.1 these were the maximum allowed degrees of freedom we allowed ourselves. Along with the fact that we would expect more degrees of freedom to complicate detection this is what we expect from $\mathcal{O}_{15}$. If higher order interactions were to be included, such as including terms of second order in

$\mathbf{v}_{\text{el}}^{\perp}$ or third order in $\mathbf{q}$, the limits for rejecting the background only hypothesis in favour of background and dark matter hypothesis would be even higher than for $\mathcal{O}_{15}$.

If we compare short-range interactions to long-range interactions one can see that the coupling constant one may discover for each dark matter particle mass is significantly larger for long-range interactions. This has to do with the dependence on a reference momentum as well as the momentum transfer for long-range interactions. The general form for the scattering amplitude (3.26) states that in order for short-range interactions to have the same scattering amplitude as long-range interactions under the same operator with $c_i^s \approx c_i^l$, we require that $q_{\text{ref}}^2/|\mathbf{q}|^2 \approx 1$. We want the scattering amplitude to be approximately equal in both cases in order to produce an equal amount of signals in the detector. The reference momentum is defined as $q_{\text{ref}} = \alpha m_e$ where $\alpha = 1/137$ and the electron mass $m_e = 0.511$ MeV. This means that the transfer momentum must be of order 10^{-3}. This sets the scale for how much the momentum transfer must compensate in order to produce a scattering amplitude that is equal in both forms of interaction. However, since the transfer momentum is determined by the properties of the dark matter particle mass and velocity distribution, the long-range coupling constant has to compensate instead, by being larger than its short-range counterpart. In Figure 6.3 this effect is slightly suppressed, since an increase in the energy range at the lower boundary means that smaller dark matter particle masses can be studied which. In turn, this means that the long-range coupling constant has to compensate less in order to produce the same number of events as the short-range interactions.

This brings us to a feature of Figure 6.3. By lowering the minimum electron recoil energy E_e from 0.2 keV to 0.02 keV we notice that the mass range is also extended. This is due to kinematics. By allowing for smaller recoil energies to be studied, we also allow light, fast dark matter particles to be taken into account. We can also see that this setup for the detector allows for smaller coupling constants to be probed even for larger masses. Since the velocity distribution of the dark matter particles is a Maxwellian, we include a larger portion of the particles in the halo to be probed by lowering the energy threshold allowing for heavier, slower dark matter particles to be detected.

It is worth noting that we could have chosen to show the sensitivities for all interaction operators listed in Table 3.1. The ones that are shown are selected because they either produce unique sensitivity regions or allow us to study the effects of a unique feature. Many interactions operators are similar to some other interaction operator, differing only in the spin operator. This is the case for e.g. operators $\mathcal{O}_3$ and $\mathcal{O}_5$. The sensitivity regions for these operators would be almost identical. Furthermore, producing the sensitivity for each operator under both long range and short range interactions would be too time consuming, and the analysis of the results would be the same. Based on all this, we selected a set of interaction operators that would display key features to be discussed in our analysis.

In the article by Catena et. al. [3] the authors show that the squared scattering

amplitude (3.53) can be written in terms of the dark matter response functions as well as the atomic response functions. In previous studies [2], only one atomic response function has been found. This atomic response function is related to the scalar form factor (3.31). By forming a more general theory of dark matter-electron interactions, however, we showed that there is also a vectorial form factor (3.33). Catena et. al. show that this produces additional atomic response functions. These new response functions are the ones that are generated by interaction operators that depend on $\mathbf{v}_{\mathrm{el}}^{\perp}$ in some way. These operators are $\mathcal{O}_3, \mathcal{O}_5, \mathcal{O}_7, \mathcal{O}_8, \mathcal{O}_{12}, \mathcal{O}_{13}, \mathcal{O}_{14}$ and $\mathcal{O}_{15}$. As the authors mention, the size of these response functions determine the actual ionisation rate that we measure. In particular, the interaction operator $\mathcal{O}_{15}$ generates a response function that effectively decreases the ionisation rate for that interaction. This adds to the reason why interactions under operator $\mathcal{O}_{15}$ require a higher sensitivity for detection.

7.3 Limitations and assumptions

The exclusion limits presented in this thesis have been simulated with a statistical significance $\mathcal{Z} = 3$. With this significance, we reject the background only hypothesis with a certainty of 99.8%. This is a good approximation, but it is still prone to some statistical fluctuations. A higher significance could be used, but this would require more time as well as more computing power.

We have also assumed the standard halo model for the velocity distribution as well as the dark matter density. While being a simple model, the standard halo is still widely used for these kinds of experiments.

This work has focused on detectors utilising a xenon target. As mentioned, there are other targets as well. DarkSide-50 was mentioned as an argon based experiment. However, since the XENON1T is being upgraded, this was seen as a more interesting venue to explore. If time had allowed, one could also have studied the sensitivity for argon based detectors.

The interactions investigated in this thesis has been simplistic, we have investigated cases where dark matter interacts with electrons under one operator alone. This incorporates a one-dimensional minimisation when we produce the test statistic for each mass. A superposition of two interaction operators would require a two-dimensional minimisation, which is too time consuming to have been included in this work.

7.4 Ideas for future studies

For future studies of the sensitivity in direct detection experiments, one can incorporate a higher statistical significance. This would make the predictions more precise. For example, a statistical significance of $\mathcal{Z} = 5$ would mean that one can reject the background only hypothesis with a certainty of 99.999943%.

Another interesting aspect would be the study of other models for the dark matter distribution. In the article by Freese et. al. [8] the authors give a more in-depth discussion on the standard halo model as well as other solutions for the velocity distribution.

As an extension of this work, one could produce sensitivity plots for argon based detectors as well. A good idea would be to use the DarkSide-50 experiment as a starting point and find the sensitivity for experiments with larger exposure.

Investigating interactions that depend on more than one operator would also be a natural extension to this work. This would mean that one could start investigating the required sensitivity for rejecting the background only hypothesis for more complex interactions, such as the anapole.

7.5 Conclusion

The aim of this thesis was to present the sensitivity required in next-generation direct detection experiments to reject the background only hypothesis, in favour of the background and dark matter hypothesis, under the assumption that dark matter interacts primarily with electrons. This has been achieved by presenting a general interaction model for dark matter-electron interactions. This model was then used to simulate event rates in direct detection experiments. Using statistical simulations, we have been able to produce the sensitivity required to reject the background only hypothesis in the future XENONnT experiment with a statistical significance $\mathcal{Z} = 3$.

Bibliography

[1] G. Bertone and D. Hooper, *A history of dark matter*, 2016. arXiv: 1605.04909 [astro-ph.CO].

[2] R. Essig, J. Mardon and T. Volansky, *Direct detection of sub-gev dark matter*, 2011. arXiv: 1108.5383 [hep-ph].

[3] R. Catena, T. Emken, N. Spaldin *et al.*, *Atomic responses to general dark matter-electron interactions*, 2019. arXiv: 1912.08204 [hep-ph].

[4] T. Emken, *Dark matter-induced atomic response code (darkarc) v1.0*, 2019. DOI: [DOI:10.5281/zenodo.3581334]. [Online]. Available: https://doi.org/10.5281/zenodo.3581334.

[5] F. Bessel, "*On the variations of the proper motions of Procyon and Sirius*", *Mon. Not. Roy. Astron. Soc.*, vol. 6, pp. 136–141, 1844.

[6] L. Kelvin, *Baltimore lectures on molecular dynamics and the wave theory of lights*, English. C.J. Clay and sons, London, 1904.

[7] F. Zwicky, "*Die Rotverschiebung von extragalaktischen Nebeln*", *Helvetica Physica Acta*, vol. 6, pp. 110–127, Jan. 1933.

[8] K. Freese, M. Lisanti and C. Savage, *Annual modulation of dark matter: A review*, 2012. arXiv: 1209.3339 [astro-ph.CO].

[9] G. Bertone, D. Hooper and J. Silk, *Particle dark matter: Evidence, candidates and constraints*, 2004. arXiv: hep-ph/0404175 [hep-ph].

[10] T. D. Collaboration, P. Agnes, I. F. M. Albuquerque *et al.*, *Constraints on sub-gev dark matter-electron scattering from the darkside-50 experiment*, 2018. arXiv: 1802.06998 [astro-ph.CO].

[11] E. Aprile, J. Aalbers, F. Agostini *et al.*, *Light dark matter search with ionization signals in xenon1t*, 2019. arXiv: 1907.11485 [hep-ex].

[12] A. L. Fitzpatrick, W. Haxton, E. Katz *et al.*, *The effective field theory of dark matter direct detection*, 2012. arXiv: 1203.3542 [hep-ph].

[13] B. A. Dobrescu and I. Mocioiu, *Spin-dependent macroscopic forces from new particle exchange*, 2006. arXiv: hep-ph/0605342 [hep-ph].

[14] J. Fan, M. Reece and L.-T. Wang, *Non-relativistic effective theory of dark matter direct detection*, 2010. arXiv: 1008.1591 [hep-ph].

[15] E. D. Nobile, G. B. Gelmini, P. Gondolo *et al.*, *Direct detection of light anapole and magnetic dipole dm*, 2014. arXiv: 1401.4508 [hep-ph].

[16] R. Catena, T. Emken and J. Ravanis, *Rejecting the majorana nature of dark matter with electron scattering experiments*, 2020. arXiv: 2003.04039 [hep-ph].

[17] M. E. Peskin and D. V. Schroeder, *An Introduction to Quantum Field Theory*. Westview Press, 1995, Reading, USA: Addison-Wesley (1995) 842 p.

[18] E. D. Nobile, M. Cirelli and P. Panci, *Tools for model-independent bounds in direct dark matter searches*, 2013. arXiv: 1307.5955 [hep-ph].

[19] R. Essig, M. Fernandez-Serra, J. Mardon *et al.*, *Direct detection of sub-gev dark matter with semiconductor targets*, 2015. arXiv: 1509.01598 [hep-ph].

[20] G. Cowan, K. Cranmer, E. Gross *et al.*, *Asymptotic formulae for likelihood-based tests of new physics*, 2010. arXiv: 1007.1727 [physics.data-an].

[21] E. Andersson, A. Bökmark, R. Catena *et al.*, *Projected sensitivity to sub-gev dark matter of next-generation semiconductor detectors*, 2020. arXiv: 2001.08910 [hep-ph].

[22] W. H. Press, S. A. Teukolsky, W. T. Vetterling *et al.*, *Numerical Recipes 3rd Edition: The Art of Scientific Computing*, 3rd ed. USA: Cambridge University Press, 2007, ISBN: 0521880688.

A
Code

Here we present all functions used to compute the results presented within this thesis. All code is written in C++ and is meant to serve as an extension of the code used in Catena et. al. [3] in addition to DarkARC [4].

A.1 `Poisson_Sample()`

Samples a set amount of points N_i from a Poisson distribution (4.2) with a mean μ_i.

```
std::vector<double> Poisson_Sample(std::vector<double> Mean, int
    length){

    // Seeds the random number generator using the internal clock
       of the system
    unsigned seed = std::chrono::system_clock::now().
       time_since_epoch().count();
    std::default_random_engine generator (seed);
    std::vector<double> Samples(length);

    for(int i = 0; i < length; i++){

        std::poisson_distribution<int> distribution(Mean[i]);

        Samples[i] = distribution(generator);

    }

    return Samples;

}
```

A.2 `negativeloglikelihood()`

Calculates the negative logarithm of the likelihood in the denominator of (4.11). Note that this is not the function `NegativeLogLikelihood()`, as this is defined within the function `Significance()`. The function defined in this section depends on several parameters, whereas the function `NegativeLogLikelihood()` depends only on the coupling constant.

```
double negativeloglikelihood(std::vector<double> N, std::vector<
    double> Fiducial_Spectrum, std::vector<double> Background,
    double coupling){

        int length = Fiducial_Spectrum.size();
        std::vector<double> Expectation_Value(length);
        double NegativeLogLikelihood_Denominator = 0.0;

        for(int i = 0; i < length; i++){

                Expectation_Value[i] = Background[i] + (coupling *
                    coupling * Fiducial_Spectrum[i]);

                NegativeLogLikelihood_Denominator =
                    NegativeLogLikelihood_Denominator + (
                    Expectation_Value[i] - N[i] * log(
                    Expectation_Value[i]));

        }

        return NegativeLogLikelihood_Denominator;

}
```

A.3 Help functions for the golden search method

The minimisation functions require a few help functions. `MAX()` compares two values and returns the larger one. `MIN()` performs a similar operation, comparing two values, but instead it returns the smaller value. `SWAP()` swaps the memory adress for two values with each other. `SIGN()` is the only non-trivial help function. It takes two values as input `a` and `b`. The function then returns the magnitude of `a` with the sign of `b`.

```
double MAX(double a, double b){

        if(a > b){

                return a;

        }
        else if(b > a){

                return b;

        }
        else{

                return a;

        }

}
```

```
double MIN(double a, double b){

        if(a > b){

                return b;

        }
        else if(b > a){

                return a;

        }
        else{

                return a;

        }

}
```

```
void SWAP(double &a, double &b){

        double c = a;
        a = b;
        b = c;

}
```

```
double SIGN(double a, double b){

        if(a < 0){

                if(b < 0){

                        return a;

                }
                else{

                        return -a;

                }

        }
        else if(b < 0){

                return -a;

        }
        else{

                return a;

        }

}
```

A.4 golden.bracket()

Struct defined in Numerical Recipes [22] that brackets the minimum for a function.

```
struct Bracketmethod{

        double ax, bx, cx, fa, fb, fc;
        template <class T>
        void bracket(const double a, const double b, T &func)
        {
                const double GOLD = 1.618034, GLIMIT = 100.0, TINY
                   = 1.0e-20;
                ax = a; bx = b;
                double fu;
                fa = func(ax);
                fb = func(bx);

                if(fb > fa){

                        SWAP(ax, bx);
                        SWAP(fb, fa);

                }

                cx = bx + GOLD * (bx - ax);
                fc = func(cx);

                while(fb > fc){

                        double r = (bx - ax) * (fb - fc);
                        double q = (bx - cx) * (fb - fa);
                        double u = bx - ((bx - cx) * q - (bx - ax)
                           * r)/(2.0 * SIGN(MAX(abs(q - r), TINY),
                           q - r));
                        double ulim = bx + GLIMIT * (cx - bx);

                        if((bx - u) * (u - cx) > 0.0){

                                fu = func(u);
                                if(fu < fc){

                                        ax = bx;
                                        bx = u;
                                        fa = fb;
                                        fb = fu;
                                        return;

                                }
                                else if(fu > fb){

                                        cx = u;
                                        fc = fu;
                                        return;

                                }
```

```
                                u = cx + GOLD * (cx - bx);
                                fu = func(u);

                        }
                        else if((cx - u) * (u - ulim) > 0.0){

                                fu = func(u);

                                if(fu < fc){

                                        shft3(bx, cx, u, u + GOLD *
                                            (u - cx));
                                        shft3(fb, fc, fu, func(u));

                                }
                        }

                        else if((u - ulim) * (ulim - cx) >= 0.0){

                                u = ulim;
                                fu = func(u);

                        }
                        else{

                                u = cx + GOLD * (cx - bx);
                                fu = func(u);

                        }

                        shft3(ax, bx, cx, u);
                        shft3(fa, fb, fc, fu);

                }
        }
        inline void shft2(double &a, double &b, const double c)
        {
                a = b;
                b = c;
        }
        inline void shft3(double &a, double &b, double &c, const
            double d)
        {
                a = b;
                b = c;
                c = d;
        }
        inline void mov3(double &a, double &b, double &c, const
            double d, const double e, const double f)
        {
                a = d;
                b = e;
                c = f;
        }
};
```

A.5 golden.minimize()

Definition of the function listed in Numerical Recipes [22] that finds the minimum of a function.

```
struct Golden:Bracketmethod{

        double xmin, fmin;
        const double tol;
        Golden(const double toll = 3.0e-3):tol(toll){}
        template <class T>
        double minimize(T &func)
        {
                const double R = 0.61803399, C = 1.0 - R;
                double x1, x2;
                double x0 = ax;
                double x3 = cx;

                if(abs(cx - bx) > abs(bx - ax)){

                        x1 = bx;
                        x2 = bx + C * (cx - bx);

                }
                else{

                        x2 = bx;
                        x1 = bx - C * (bx - ax);

                }

                double f1 = func(x1);
                double f2 = func(x2);

                while(abs(x3 - x0) > tol * (abs(x1) + abs(x2))){

                        if(f2 < f1){

                                shft3(x0, x1, x2, R * x2 + C * x3);
                                shft2(f1, f2, func(x2));

                        }
                        else{

                                shft3(x3, x2, x1, R * x1 + C * x0);
                                shft2(f2, f1, func(x1));

                        }
                }

                if(f1 < f2){

                        xmin = x1;
                        fmin = f1;
```

```
                }
                else{

                                xmin = x2;
                                fmin = f2;

                }
                return xmin;
        }
};
```

A.6 Significance()

Evaluates the statistical significance $\mathcal{Z}$ for a given data set.

```
double Significance(double mass, double coupling, Atom& atom){

        // Initial brackets for Golden search
        double a = 0.0, b = 1.0;

        // Calls the function that searches for the minimum
        Golden golden;

        // Set the DM mass (MeV)
        DM_Particle DM(mass * MeV);

        // Seed the poisson random number generator
        unsigned seed = std::chrono::system_clock::now().
            time_since_epoch().count();
        std::default_random_engine generator(seed);

        // Set initial values
        int Max_Iterations = 20; // Set maximum number of
            iterations = number of energy bins
        int Max_q = 1000; // Set amount of q-values

        double E_1;
        double E_2;
        double E_min = 0.2 * keV; // Minimum energy
        double E_max = 3.0 * keV; // Defines size of each bin, and
            along with max iterations max energy
        double Step_Length = (E_max - E_min)/Max_Iterations; //
            Energy bin size
        double exposure = 4.0 * 22.0 * 1000.0 * kg * day; //
            Exposure four times that of XENON1T
        double Background_Value = 1.0/(1000.0 * kg * day * keV); //
             Amount of background signals

        // Make vectors
        std::vector<double> Energy_Bins(Max_Iterations); // Stores
            the middle energy value in each bin
        std::vector<double> Fiducial_Spectrum(Max_Iterations); //
            Stores the DM signals in each bin
```

```
        std::vector<double> Expectation_Value(Max_Iterations); //
            Stores background + signal
        std::vector<double> Background(Max_Iterations); // Stores
            the background signal in each bin
        std::vector<double> N_NullHypothesis(Max_Iterations); //
            Stores N_values for nullhypothesis
        std::vector<double> N_AlternativeHypothesis(Max_Iterations)
            ; // N_values for alt-hypothesis
        std::vector<double> Likelihood_NullHypothesis_Numerator(
            Max_q);
        std::vector<double>
            Likelihood_AlternativeHypothesis_Numerator(Max_q);
        std::vector<double> q_Null(Max_q); // Stores the q-values
            for nullhypothesis
        std::vector<double> q_Alternative(Max_q); // Stores q_alt

        // Set the background in each bin
        for(int i = 0; i < Max_Iterations; i++){

                Background[i] = Background_Value * exposure *
                    Step_Length;

        }

        // Loop over j, each value of j corresponds to a q-value
        for(int j = 0; j < Max_q; j++){

                //Set the couplings
                DM.Reset_Couplings();           // Sets all
                    couplings to zero
                DM.Set_Coupling(13, 0.0, 1.0);  // Arguments: (
                    operator, contact interaction, long range
                    interaction)

                // Loop over energy bins
                for(int i = 0; i < Max_Iterations; i++){

                        E_1 = E_min + i * Step_Length;
                        E_2 = E_min + (i + 1) * Step_Length;
                        Energy_Bins[i] = E_2 - (Step_Length/2); //
                            Find the centre of each bin
                        Fiducial_Spectrum[i] = Number_Of_Events(DM,
                             atom, E_1, E_2, exposure); // Fiducial
                            Spectrum

                }

                // Produce the expectation value
                for(int i = 0; i < Max_Iterations; i++){

                        Expectation_Value[i] = Background[i] + (
                            coupling * coupling * Fiducial_Spectrum[
                            i]);

                }
```

```
                // Save_List("../results/Background.txt",Background
                    );
                // Save_List("../results/Expectationvalues.txt",
                    Expectation_Value);

                // Sample values from Poisson distribution
                N_NullHypothesis = Poisson_Sample(Background,
                    Max_Iterations);
                N_AlternativeHypothesis = Poisson_Sample(
                    Expectation_Value, Max_Iterations);

                ///// Null Hypothesis /////
                // Make the function NegativeLogLikelihood() that
                    only depends on the coupling constant
                std::function<double(double)> NegativeLogLikelihood
                     = [&N_NullHypothesis, &Fiducial_Spectrum, &
                    Background](double c){

                        return negativeloglikelihood(
                            N_NullHypothesis,Fiducial_Spectrum,
                            Background,c);

                };

                // Minimise the negative log-likelihood for the
                    nullhypothesis
                golden.bracket(a,b,NegativeLogLikelihood);
                double c_Null_Max = golden.minimize(
                    NegativeLogLikelihood);
                double Likelihood_Null_Max = -1.0 *
                    NegativeLogLikelihood(c_Null_Max);

                ///// Alternative Hypothesis /////
                NegativeLogLikelihood = [&N_AlternativeHypothesis,
                    &Fiducial_Spectrum, &Background](double c){

                        return negativeloglikelihood(
                            N_AlternativeHypothesis,
                            Fiducial_Spectrum,Background,c);

                };

                // Minimise the negative log-likelihood for the
                    alternative hypothesis
                golden.bracket(a,b,NegativeLogLikelihood);
                double c_Alt_Max = golden.minimize(
                    NegativeLogLikelihood);
                double Likelihood_Alt_Max = -1.0 *
                    NegativeLogLikelihood(c_Alt_Max);

                // Find the likelihood numerators
                Likelihood_NullHypothesis_Numerator[j] = 0.0;
                Likelihood_AlternativeHypothesis_Numerator[j] =
                    0.0;

                for(int i = 0; i < Max_Iterations; i++){
```

```
                    Likelihood_NullHypothesis_Numerator[j] =
                        Likelihood_NullHypothesis_Numerator[j] +
                         (Background[i] - N_NullHypothesis[i] *
                        log(Background[i]));
                    Likelihood_AlternativeHypothesis_Numerator[
                        j] =
                        Likelihood_AlternativeHypothesis_Numerator
                        [j] + (Background[i] -
                        N_AlternativeHypothesis[i] * log(
                        Background[i]));

            }

            // Fixes the sign
            Likelihood_NullHypothesis_Numerator[j] = -1.0 *
                Likelihood_NullHypothesis_Numerator[j];
            Likelihood_AlternativeHypothesis_Numerator[j] =
                -1.0 *
                Likelihood_AlternativeHypothesis_Numerator[j];

            // Store the q-values for both hypotheses
            q_Null[j] = -2 * (
                Likelihood_NullHypothesis_Numerator[j] -
                Likelihood_Null_Max);
            q_Alternative[j] = -2 * (
                Likelihood_AlternativeHypothesis_Numerator[j] -
                Likelihood_Alt_Max);

    } // End of loop over j

    ///// Find Z /////

    // Sort the list so that the smallest number is first, and
        largest number is last
    std::sort(q_Alternative.begin(), q_Alternative.end());

    // Find the median of the distribution for q_Alternative
    double Median_q_Alternative;
    if(q_Alternative.size() % 2 == 0){

            Median_q_Alternative = (q_Alternative[q_Alternative
                .size()/2] + q_Alternative[q_Alternative.size()
                /2 - 1])/2.0;

    }
    else{

            Median_q_Alternative = q_Alternative[q_Alternative.
                size()/2];

    }

    // Return the statistical significance Z
    return sqrt(Median_q_Alternative);
```

```
}
```

A.7 The main function

The main function which uses `Significance()` as well as `Find_Root()` defined previously [3] to produce the sensitivity for experiments.

```
using namespace std::chrono;

int main(int argc, char *argv[]){

        auto Time_Start = steady_clock::now();

        Atom Argon = Import_Electronic_Responses("Ar");
        Atom Xenon = Import_Electronic_Responses("Xe");

        // Create vectors for storing masses and coupling constants
        std::vector<double> mass(50);
        std::vector<double> c(50);

        // Loop over the masses
        for(int i = 1; i < 51; i++){

                // This if-statement is here in order to spread out
                    the masses, when plotting on a log scale the
                   lower masses are the ones where higher
                   resolution is more interesting

                // For the low energy threshold
                if(i < 21){

                        mass[i - 1] = 10.0 + 2.0 * (i - 1);

                }

                else if(i < 31){

                        mass[i - 1] = 50.0 + 20.0 * (i - 21);

                }

                else{

                        mass[i - 1] = 250.0 + 87.0 * (i - 31);

                }

/*               // For the high energy threshold (XENONnT)
                if(i < 11){

                        mass[i - 1] = 65.0 + 3.0 * (i - 1);

                }
```

```
                else if(i < 21){

                        mass[i - 1] = 100.0 + 20.0 * (i - 10);

                }

                else{

                        mass[i - 1] = 350.0 + 88.0 * (i - 20);

                }
*/
                // For checking a specific mass
                // mass[i - 1] = 300.0;

                // Mass given in MeV
                double m = mass[i - 1];

                // Defines the function that is used in Find_Root()
                std::function<double(double)> significance = [m, &
                    Xenon](double coupling){

                        return Significance(m, coupling, Xenon) -
                            3.0;

                };

                // Calls the function that finds the root of Z-3
                c[i - 1] = Find_Root(significance, 1.0e-8, 1.0e-3,
                    1.0e-12); // Arguments: (lower boundary, upper
                    boundary, precision for c)

        }

                //Ending time and computing time
                auto Time_End = steady_clock::now();
                double durationTotal =1e-6 * duration_cast<
                    microseconds>(Time_End - Time_Start).count();
                std::cout <<"\nProcessing Time:\t"<< durationTotal
                    <<"s ("<< floor(durationTotal/3600.0)<<":"<<
                    floor(fmod(durationTotal/60.0, 60.0))<<":"<<
                    floor(fmod(durationTotal, 60.0))<<":"<<floor(
                    fmod(1000 * durationTotal, 1000.0))<<")."<<std::
                    endl;

        return 0;
}
```